Mechanical Systems and Signal Processing 120 (2019) 422–448

Contents lists available at ScienceDirect

Mechanical Systems and Signal Processing

journal homepage: www.elsevier.com/locate/ymssp

Acoustic beamforming for noise source localization – Reviews, methodology and applications

Paolo Chiariotti [a], Milena Martarelli [b], Paolo Castellini [a,*]

[a] Università Politecnica delle Marche Politecnica delle Marche, Via Brecce Bianche, 60131 Ancona, Italy
[b] Università degli Studi e-Campus, Via Isimbardi, Novedrate, CO, Italy

ARTICLE INFO

Article history:
Received 25 August 2017
Received in revised form 5 August 2018
Accepted 16 September 2018
Available online 31 October 2018

Keywords:
Acoustic beamforming
Acoustic imaging techniques
Noise source localization
Microphone arrays
Acoustic measurements

ABSTRACT

This paper is a review on acoustic beamforming for noise source localization and its applications. The main concepts of beamforming, starting from the very basics and progressing on to more advanced concepts and techniques, are presented, in order to give the reader the possibility to identify concepts and references which might be useful for her/his work. Practical examples referring to application of this technique in different scenarios are also provided. The aim is to make the reader comfortable with the topic and aware of the wide stimuli a technique like acoustic beamforming can offer researchers.

1. Introduction

The term *Beamforming* refers to a data processing method for spatially filtering signals coming from an array of sensors. This spatial selectivity becomes possible by mathematically steering (or focusing, depending on the source-receiver relative distance) the array on a preferential direction. The application fields of this technique range from radio to seismic and sound waves. When dealing with the latter, the term *acoustic beamforming* is often used. However, a first clarification is needed. Indeed, there are two main branches of acoustic beamforming, the one related to *signal extraction* and the one addressing *source localization*. This paper focuses on the latter working field. The reader might refer to the interesting paper of Gannot et al. [1] for understanding how beamforming can be exploited for signal extraction. The initial idea of beamforming was mathematically formalized, both in the time and in frequency domains, by Billingsley et Al. in 1974–1976. Since Billingsley's *acoustic telescope* [2], acoustic beamforming has experienced a dramatic improvement over the years because of the advancement in data acquisition and processing capabilities. One of these improvements related to sound source localization was, for example, the coupling with a video-camera (*acoustic camera*) [3]. Due to these constant improvements, it has been difficult to provide a comprehensive literature review on this subject. Michel [4] tried to do that by presenting, in 2006, a paper reviewing the recent history of acoustic beamforming; however he focused more on the different application fields that could be tackled by acoustic beamforming, or phased arrays in general, and gave just a hint of more complex processing approaches like deconvolution. After a decade, this paper aims at presenting the subject from a different point of view with respect to Michel's work; in fact, this review aims more at collecting and discussing the different strategies that have contributed to create the research field of acoustic beamforming for noise source localization, i.e. tackling direct, inverse, decon-

* Corresponding author.
E-mail address: p.castellini@univpm.it (P. Castellini).

https://doi.org/10.1016/j.ymssp.2018.09.019
0888-3270/

volution and spherical harmonic methods among others, and providing some technical details on how to set-up a beamforming test.

The paper is organized as follows: Section 2 introduces a brief history and the key concepts of acoustic beamforming; Section 3 addresses the topic of microphone array design, with a special focus on performance, array calibration and associated uncertainty; a general description of several beamforming strategies is provided in Section 4, while Section 5 illustrates the most established applications of acoustic beamforming; Section 6 draws the main conclusions of the work.

2. Brief history and basic concept of beamforming

Acoustic beamforming is a signal processing technique based on far-field microphone array measurements. While an array produces a spatial sampling of a sound field, a beamforming algorithm performs a spatial filtering operation that makes it possible to map the distribution of the sources at a certain distance from the array and therefore locate the strongest sources. Indeed beamforming algorithms enhance the signal-capturing capabilities of the array in a particular direction, giving rise to a steered signal, i.e. the *beamformer*, that is stronger when the steering direction is closer to the propagating direction of the source.

The first documented beamforming solution dates back to the 1940s [5] and relates to the development of a radio antenna for military applications, i.e. a "direction finder used in submarine detection". For almost 20 years beamforming was applied to radio signals [6] and in steerable source antennas [7]. In the 1970s it was also applied in seismic arrays [8] and finally in acoustics [2]. After the work of Billingsley, in 1977 Fisher et Al. came up with a similar concept and named it as the "polar correlation" method [9]. A comparison of the two approaches was then performed by Billingsley in [10]. Over the following years, different algorithms and approaches have been developed, whose level of complexity has also increased, benefiting from the improvement in data acquisition and computer computation performances. Most of these algorithms will be presented in the following sections of this paper, nevertheless it might be here beneficial to provide some basic concepts of beamforming by presenting the so-called Delay-and-Sum (D&S) approach in the time domain.

Like all beamforming algorithms, D&S too relies on a source-receiver dependence. Whether the receivers are in the far-field or in the near-field with respect to the source, the D&S algorithm seeks phase delay by virtually *steering* or *focusing* the array towards a particular direction (plane wave propagation) or a particular point in space (spherical wave propagation). Considering the latter situation, let's consider two main actors: a grid of *N*points (control points) each located at $\vec{x}_p, p = 1 \dots N$, in which a set of candidate sources (usually monopoles) can be virtually placed, and a discrete set of *M*microphones that sample the sound field and are each located at $\vec{x}_m, m = 1 \dots M$. For convenience's sake, the origin of the coordinate system can be considered to coincide with the *phase center* of the array, yielding $\sum_{m=1}^{M} \vec{x}_m = 0$. Each time signal recorded by each microphone of the array is back–propagated to each control point by taking into account the relative control point–receiver position in space and the propagation velocity of the acoustic wave in the medium considered. In fact, these two terms provide the time delay (or phase shift) to be taken into account when virtually focusing the array towards a certain control point. The delayed data are then summed yielding the *beamformer* output associated to that control point. If a source is present on a control point, the delayed signals turn out to be cophased and the beamformer output is maximized. When focusing on an arbitrary control point, different from where the source is located, the signals are not cophased, thus resulting in a lower output than the one produced where the source is located. The whole concept is graphically illustrated in Fig. 1, together with its optical analogy. The beamformer response $\mathrm{bf}(p,t)$ at the p^{th} control point and at the t^{th} time instant can be calculated using

$$\mathrm{bf}(\vec{x}_p, t) = \frac{1}{M} \sum_{m=1}^{M} w_m A_m(\vec{x}_p, \vec{x}_m) p_m\left(t - \frac{|\vec{x}_p - \vec{x}_m|}{c}\right) \tag{1}$$

where:

- p_m is the pressure signal at the m^{th} microphone;
- w_m is a weighting factor or shading coefficient applied to the individual m^{th} microphone
- $A_m(\vec{x}_p, \vec{x}_m)$ is a scaling factor, which can also take into account amplitude reduction. i.e. $A_m(\vec{x}_p, \vec{x}_m) = 4\pi\|\vec{x}_p - \vec{x}_m\|$;
- c is the wave propagation speed in the medium.

The sound pressures measured at each $\vec{x}_m$ location are weighted, scaled and delayed, according to the relative distance between each microphone and the p^{th} control point considered, and then summed up to give the beamformer output, hence the name Delay & Sum Beamforming. The performance of the whole method is highly related to the weighting function, since the w_m term is influenced by the array pattern, the beam pattern and the Point Spread Function (PSF). All these latter concepts will be discussed in depth in Section 3.

The time domain beamforming equation can be also translated into frequency domain. The first author to present beamforming in the frequency domain was Williams [11], who highlighted the analogy "between the formation of sequential beams in a line array and the fast Fourier transform". The frequency domain representation of D&S beamforming is illustrated in

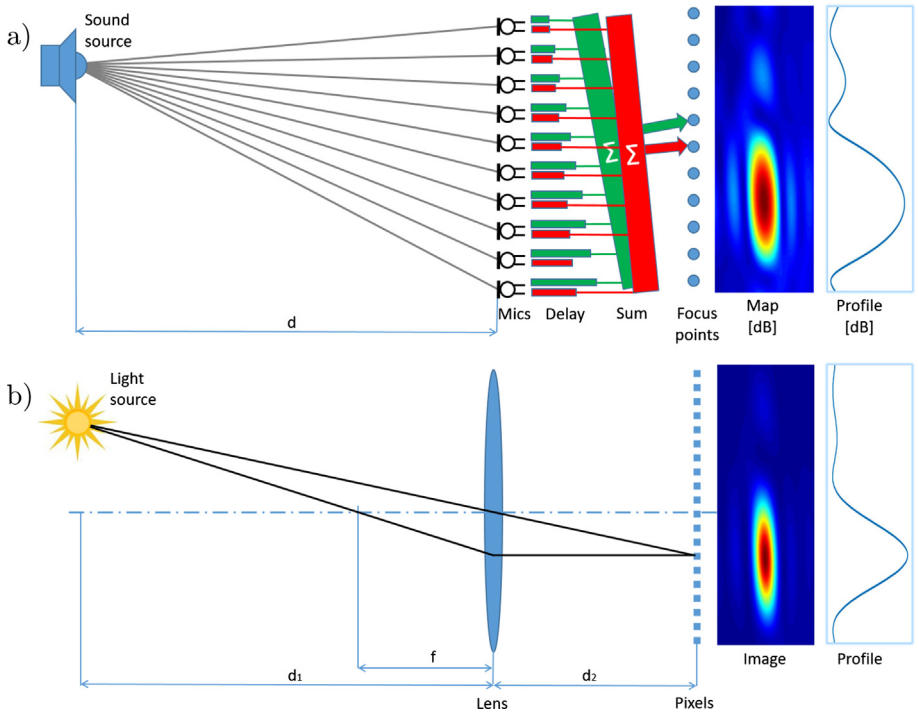

Fig. 1. Sound "camera" model a) and optical camera model b).

$$\mathrm{BF}(\vec{x}_p,\omega_k)=\frac{1}{M}\sum_{m=1}^{M}w_m A_m(\vec{x}_p,\vec{x}_m)P_m(\omega_k)e^{j\omega_k\frac{|\vec{x}_p-\vec{x}_m|}{c}} \tag{2}$$

where $P_m(\omega_k)$ is the pressure signal at the m^{th} microphone and at the angular frequency ω_k.

Eq. (2) can also be reformulated using vector-matrix notation, thus yielding

$$\mathrm{BF}(\vec{x}_p,\omega_k)=\mathbf{g}^{\mathrm{H}}\mathbf{W}\mathbf{p}. \tag{3}$$

The term **g** in Eq. (3) is commonly called the *steering vector*, since it contains phasors whose exponents cancel wave propagation related phase shifts. It is common to include the scaling factor A_m in the steering vector notation. The term **p** is a vector whose elements are the complex pressures $P_m(\omega_k)$ measured at each microphone location, while the matrix **W** is a diagonal matrix whose elements are the weighting factors. The superscript $^{\mathrm{H}}$ represents the complex conjugate transpose operator.

3. Beamforming test design criteria

When designing a beamforming test there are certain criteria that should be taken into account in order to maximize the expected results with respect to the application requirements. Indeed, these can be grouped in five items:

i. microphone array performance;
ii. microphone array design (also considering its influence on the acoustic field, i.e. acoustically transparent vs diffractive array);
iii. microphone array calibration;
iv. uncertainty assessment;
v. hardware metrological performance and efficiency.

An in-depth review of these concepts is out of the scope of this paper, since more detailed explanations of these themes can be found in books like [12]. The first four items will be briefly discussed in the following. The latter item will not be recalled in this document, for two main reasons: first of all, this theme is quite application-dependent and second it has already been exhaustively tackled in literature. An example of such analysis can be found, for instance, in [13], where the choice of hardware components, such as microphones, cabling and sampling boards is widely investigated for different kinds of aeroacoustic applications.

3.1. Array performance parameters

The directional sensitivity of the array-beamforming algorithm gives rise to a directivity pattern where some typical structures can be recognized: there is always a main beam pointing towards the source location, the *mainlobe*, together with other secondary beams, *sidelobes*, which are smaller in amplitude, and do not correspond to any direction/location in which the array was effectively steered/focused to. Sidelobes therefore provide information regarding the ability to filter out unwanted signals propagating from other directions.

This holding, the main performance parameters influenced by the array design are:

- Resolution
- Maximum Sidelobe Levels (MSL) and Mainlobe-to-Sidelobe Ratio (MSR)
- Spatial aliasing
- Co-array and *F* parameter
- Point Spread Function (PSF)

3.1.1. Resolution

Resolution represents the ability of the beamforming system to resolve, i.e. separate, sources close to each other by quantifying either the smallest angular separation, when dealing with sources in the far field, or the minimum distance between them, when focusing on sources at a finite distance from the array. The *Rayleigh criterion*, commonly used in array signal processing, states that two incoherent sources from different directions can be exactly resolved when the peak of the aperture smoothing function due to one source falls on the first zero of the aperture smoothing function due to the other. Considering two unit amplitude plane waves with wave numbers $\mathbf{k}_1$ and $\mathbf{k}_2$ impinging on an array with a given aperture smoothing function, and assuming that the required angular separation between sources is small at a finite distance (z), the minimum resolvable source separation, $\mathrm{R}(\theta)$, is given by

$$\mathrm{R}(\theta) = \frac{zR_k\lambda}{2\pi}\frac{1}{\cos^3(\theta)} \tag{4}$$

where:

- R_k is the distance, in the wavenumber plane, between the main peak and the first minimum value of the array pattern, according to the *Rayleigh criterion*; this term is also called the *main lobe width* in the array pattern;
- θ is the off-axis angle;
- λ is the acoustic wavelength;
- $k = \frac{2\pi}{\lambda}$ is the wavenumber.

For on-axis incidence, i.e. $\theta = 0^\circ$, the main lobe width becomes

$$R_{k,\theta=0^\circ} = a\frac{2\pi}{D} \tag{5}$$

where a is 1 for a linear aperture and 1.44 for a circular aperture, while $D$is the width of a linear aperture and the diameter of a circular aperture.

In this case the minimum resolvable source separation is given by:

$$\mathrm{R}(\theta)_{\theta=0^\circ} = a\frac{z\lambda}{D}. \tag{6}$$

A last consideration should be made regarding depth resolution. These concepts hold for near-field beamforming only. Since the beamformer focuses on a control point that is at a fixed location in space, it has the ability to resolve source location in three dimensions. However, the performance in resolving a source position in a direction perpendicular to the array (depth) is far lower than the lateral resolution capability, unless the microphone array arrangement encloses the source region under analysis. If considering a planar array and if comparing lateral to depth resolution, an ellipsoid having the major axis along the depth direction is obtained. It is quite common to have an ellipsoid characterized by a major axis to minor axis ratio up to five, thus proving the worse performance in resolving depth location.

3.1.2. Maximum Sidelobe Levels (MSL) or Mainlobe-to-Sidelobe Ratio (MSR)

The MSL parameter measures the ability of the array to reject sources coming from directions where the array is not steered/focused to. Sidelobes in the array pattern are local maxima from non-focus directions that will produce false peaks/-sources in the acoustic map. The MSL parameter therefore measures the strength of the highest sidelobe. It is clear that a good phased array should show a low MSL relative to the main lobe level. As an example, in an array with $n$randomly distributed microphones, the average sidelobes level is $1/n$ of the mainlobe strength [14], thus giving an MSL [15] of about

$$\mathrm{MSL} = -10 \cdot log\frac{1}{n}. \tag{7}$$

The Mainlobe-to-Sidelobe Ratio (MSR) expresses the ratio of the height of the mainlobe with the most important sidelobe. It is common to normalize the array pattern and to transform it into logarithmic scale, so as to display the peak of the mainlobe as 0 dB, while sidelobes at some dB down from the mainlobe. In this way, the MSR is simply the difference between the mainlobe and the strongest sidelobe.

3.1.3. Spatial aliasing

Spatial aliasing occurs when the aperture of the array is not adequately sampled in space by the sensors for a given wavelength. It is the same effect occurring in the time domain when the sampling frequency does not satisfy Shannon's theorem. However, if time domain aliasing error can be avoided by applying anti-aliasing filters, an analogous process cannot apply in spatial domain. A spatial undersampling of the array aperture results in the inability to distinguish between multiple directions of arrival. In an acoustic map, this effect yields ghost sources of levels similar as the true sources. Severe aliasing problem always occurs in regular arrays (e.g. square lattice arrays), also called redundant arrays, because of the repeated sampling spacing. One option to reduce spatial aliasing is to spatially sample at an interval that does not exceed one-half wavelength (Nyquist rate). Since this is sometimes impractical because of the considerable sensor count to meet the Nyquist criterion, other options are adopted. Indeed, in order to significantly reduce spatial aliasing, microphone arrays must guarantee *non-redundancy* in spatial sampling. This can be achieved by using non-redundant arrays with almost unique intra–sensor spacings (also known as vector spacings). This strategy leads to the class of arrays known as irregular or aperiodic arrays.

3.1.4. Co-array and F parameter

The plot of the sensors vector spacing is called *co-array* [16]. It describes the morphology of the array, rather its angular response [16,17]. Given an array of *M*microphones, if the m^{th} microphone coordinate vector is $\vec{x}_m$ the co-array of the array is obtained by

$$\vec{X} = \vec{x}_m - \vec{x}_n, m = 1 \ldots M, n = 1 \ldots M, \tag{8}$$

that is a vectorial matrix of dimension $M \times M$. Non-redundancy of the array can be measured as the number of different vector spacings U, i.e. the number of different elements in the co-array matrix. Correspondingly, non-redundancy of the array can be seen as the maximum number U_{max} of unique vectors in the co-array matrix and it is given by

$$U_{max} = M^2 - (M-1). \tag{9}$$

A synthetic index of array quality, i.e. a figure of merit, even if not fully comprehensive, is given by the percentage of unicity F, i.e. the ratio between the actual number of unique vector spacing and the maximum one

$$F = \frac{U}{U_{max}} = \frac{U}{M^2 - (M-1)} \leqslant 1. \tag{10}$$

It is clear that for an optimal irregular array it holds $F = 1$, since the number of unique vector spacings is maximized.

3.1.5. Point spread function

The output of a beamforming algorithm like D&S (Eq. 1) can be interpreted as a convolution of the real source distribution with a Point Spread Function (PSF) [18]. The PSF, which depends on the characteristics of both control points and array, represents the impulse response function of a focused imaging system and provides information on how the control points-array system blurs the source propagating to the sensors. Since the PSF is indeed an impulse response, it can be obtained by virtually placing a monopole source at a certain control point location $\vec{x}_p$ and then calculating the beamformer output for that source. It should be highlighted that the PSF is *not shift-invariant*, i.e. it is not independent of the position of the virtual source on the control points. For this reason it is important to calculate the PSF for a given set-up (control points to array arrangement). In certain cases, e.g. when the source region is small compared with the distance from the array, it is possible to assume the PSF to be shift-invariant.

3.2. Microphone array design

Two array categories will be discussed in the following subsections: acoustically transparent and diffractive arrays.

3.2.1. Acoustically transparent arrays

An acoustically transparent array usually consists of a series of omni-directional microphones located on a wire-frame like structure. The acoustically transparent condition is achieved if microphones, cables and mounting supports do not affect the sound field wherein the array is located. This arrangement is relatively easy to achieve for mid to low frequencies applications, while it becomes more complicated where very high frequency sound fields are analyzed (e.g. above 50 kHz). The wire-frame structure is definitely the commonest structure used in beamforming tests. It should also be recalled that differ-

ent arrangements might be possible, ranging from planar arrays (two-dimensional arrays), to non-planar, i.e. three dimensional shaped arrays or multi-surface arrays. The key concepts presented hereafter refer to the first category of arrays, i.e. two-dimensional arrays, even though an extension to more complex 3D shapes is quite straightforward.

The primary challenge in designing an array is to define the boundaries in terms of working frequency range. A crucial parameter is the size of the array, as discussed in [19]. The aperture size of the array, d_0, determines the lowest frequency that can be observed with an adequate resolution, or, vice versa, the resolution for a given wavelength. It is important to stress that size is intended in the direction of wave propagation for a source located in the far-field; this means that, in case of sources impinging on the array with a given angle θ with respect to the array normal, the effective aperture dimension d_{θ_f}, can be expressed as

$$d_{\theta_f} = d_0 \cos\theta. \tag{11}$$

If the source is located in the near-field with respect to the array, e.g. at a point (x_s, y_s) expressed in a reference system having the origin at the center of the array, the effective aperture dimension d_{θ_n} is obtained considering

$$d_{\theta_n} = 2\pi\sqrt{x_s^2 + y_s^2}\left[\frac{\frac{\pi}{2} - \tan^{-1}\left(\frac{y_s}{x_s + d_0/2}\right) - \tan^{-1}\left(\frac{x_s - d_0/2}{y_s}\right)}{2}\right]. \tag{12}$$

The intra-sensor spacing determines the array high frequency behavior: the smaller the intra-sensor spacing the higher the frequency that can be resolved without incurring in spatial aliasing issues. The combination of array size and intra-sensor spacing, and available acquisition channels, determine the number of sensors to be mounted on the array.

As discussed in Section 3.1, beamforming arrays are required to be non-redundant in order to reduce spatial aliasing, and for this reason regular arrays are commonly not considered. Moreover circular symmetry, also referred to as a rotational symmetry, which means that trough a rotation of $2\pi/n, n \in \mathbb{N}$, the array will cover itself or be in an identical position, is often sought in order to avoid azimuthal dependency of the map resolution. All these concepts, together with practical and economic constraints, drive the design of the array, in which the microphone locations should be defined exploiting mathematical optimization procedures. A rough classification of beamforming arrays considers the following arrangements:

- geometrical (e.g. lattice, cross–shaped, circular, etc.);
- sparse;
- random;
- spiral;
- nested.

Some common array layouts are illustrated in Fig. 2, while a performance comparison for some of the array geometries cited above is given in [20].

Geometrical arrays are the ones where sensors are arranged on simple geometrical shapes, as cross [21] or circular/multi-circle shapes [22,23]. These arrays are simple to build and present good scores in terms of figure of merit (e.g. *F*parameter) but the intrinsic geometrical regularity causes aliasing and ghost patterns in the acoustic maps. Some strategies based on signal processing can be adopted to improve the localization performance of such arrays, as the one based on a modification of the cross-spectral matrix formulation proposed by Elias in [24] for cross-shaped arrays.

Sparse arrays [25] are obtained starting from regular array, as lattice arrays, and removing the microphones so as to obtain unique intra-sensor spacings. This can reduce redundancy, but residual spurious sidelobes remain, due to spacing periodicity. A better minimization of spurious sidelobes can be obtained by random arrays, which were extensively discussed in [15]. Like other a-periodic arrays, random arrays make it possible to avoid aliasing problems and significantly reduce systematic patterns in acoustic maps. However MSL and sidelobes levels are not optimal if a limited number of sensors is utilized. Moreover, the improvement of random design for a given frequency range can be a tedious trial and error procedure and might require complex numerical optimization. The spiral design seems to be the one that found the greatest interest for its performances. Several kinds of spiral arrangements can be cited among this category of arrays:

- Archimedean
- Dougherty log-spiral [26]
- Arcondoulis spiral [27]
- Multi-arm spiral [28]

A complete comparison between six different kinds of spirals was presented by Prime and Dolan in [29]. The main advantages of spiral arrays are their ability to cover large apertures with quite few sensors, low MSL in a wide range of frequencies and good circular symmetry. Spiral arrays can be parametrically optimized according to the test case requirements and they guarantee zero-redundancy and a broad base of intra-microphone vector spacing. They are often exploited in aeroacoustic applications. The interested reader might refer to [13] to verify the performance of an Underbrink spiral array with about 100 sensors reaching a dynamic range of 12 dB in a frequency range of 1–80 kHz.

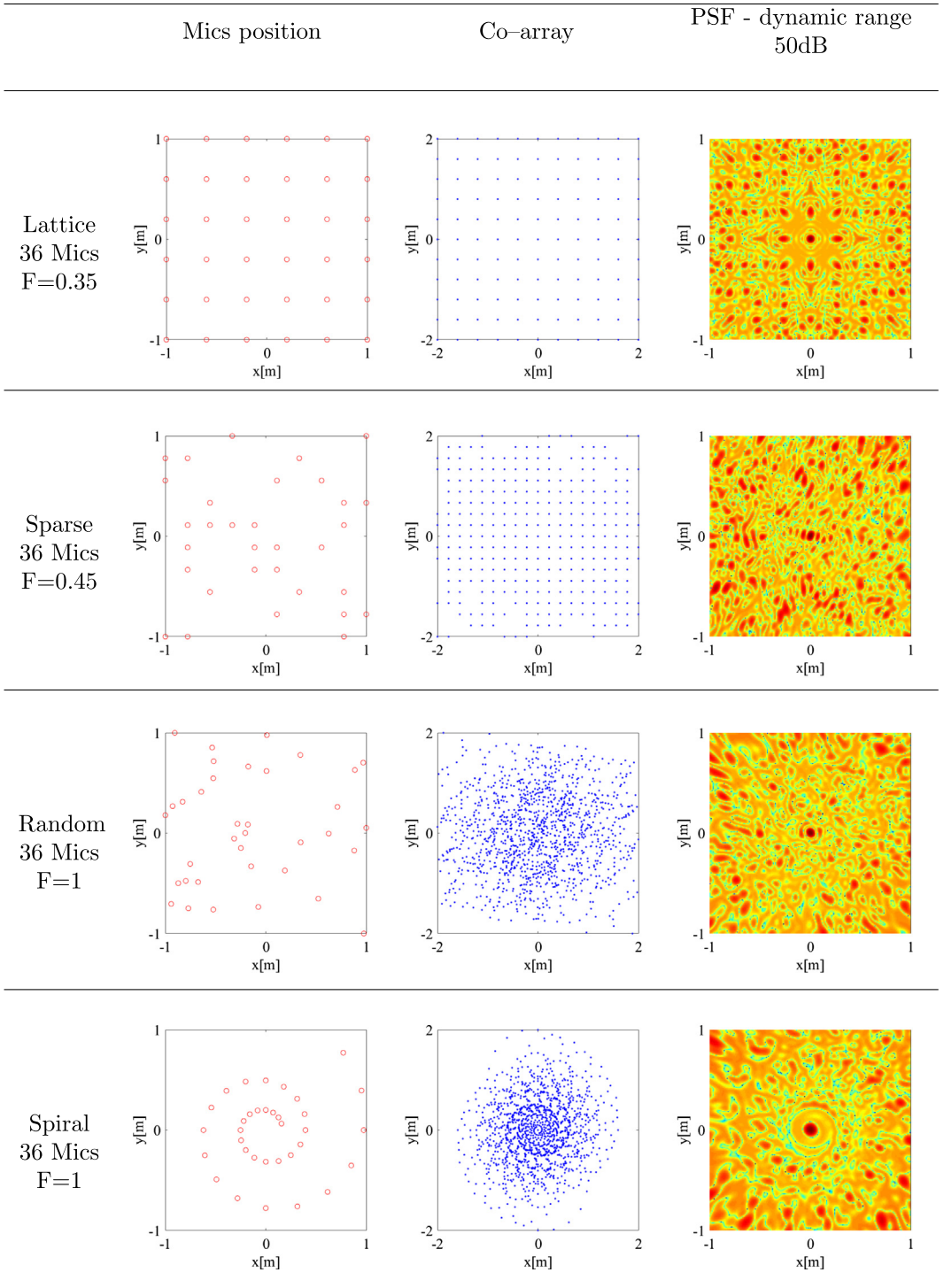

Fig. 2. Comparison between different array lay-outs.

An alternative geometric solution, which can be partially connected to a multi-arm spiral array, was proposed by Christensen et al. in [30]. Their solution is based on the utilization of an odd number of linear sub-arrays in a circularly symmetric arrangement around a common center, in which transducer positions are optimized in order to achieve non-redundancy.

When a high dynamic range is required in a large frequency range, the most suitable approach is to use nested arrays. A nested array is the combination, within the same structure, of a small array, optimized for the high frequency range, and a

large array, optimized for the low frequency range. Those arrays can be either independent or can share some sensors. In this way the size and the shape of the array can be set as the most effective for each frequency range, with an improvement of the frequency ratio from 10:1 up to 100:1.

Very recently Sarradj [31] presented a versatile approach to design arrays that can take into account uniform/non-uniform weighting without any mathematical optimization requirement. Indeed, with this solution, the microphones weights are not determined a-priori, but are tunable for the specific application. Another solution that is worth mentioning is that of moving arrays proposed by Cigada et al. in [32]. They propose to continuously change the microphones locations, by moving the array, to sample the acoustic field from different positions. Even though this strategy significantly reduces aliasing for a given number of sensors, it can be exploited if and only if the sound field is stationary.

3.2.2. Acoustically diffractive arrays

Planar arrays cannot be exploited to separate sources in–front of and behind the antenna. This makes them unusable in closed environments where a 3D source localization is to be performed. In these environments 3D shaped arrays should be exploited instead. The spherical arrangement is definitely the mostly utilized one. Even though transparent/open sphere solutions have been presented over the years [33,34], the diffractive, solid sphere arrangement definitely results the mostly exploited one. Indeed, the diffractive action of the sphere [35] (see Fig. 3) makes it possible to better separate waves propagating from different directions [36]. Microphones are flush-mounted on a rigid spherical surface shell, whose inner cavity also becomes the housing for microphones cables.

Two main advantages of the solid solution with respect to the open one can be claimed. In the low frequency range, even though the pressure level measured by a microphone placed at a point on the solid sphere does not differ too much from the level measured in a diametrically opposite position (approximately 3 dB difference), the phase difference is greater since the acoustic wave has to travel a longer distance. This increased phase difference results in an improved spatial resolution, since the sphere behaves as an acoustic lens. In the high frequency range, a masking effect takes place, and the consequent weighting of pressure data improves the directivity of the antenna. The diffractive effect has to be taken into account during data processing, and typically requires the exploitation of Spherical Harmonics Decomposition (SHD) [37]. An in–depth review of processing methods based on SHD will be discussed in Section 4.4. The influence of microphone placements over the sphere on data processing will be also commented in the same section.

3.3. Array calibration

When dealing with acoustic beamforming, three calibration steps should be considered:

- microphone sensitivity calibration;
- array calibration;
- in-situ calibration.

Microphone sensitivity calibration consists in the standard measurement of microphone sensitivity using the pressure comparison method described in IEC 61094-5, in which each microphone is fed with a known broadband or single frequency pressure level.

Microphone array calibration has the main objectives of labeling each microphone channel, assessing and correcting the inter-microphone phase delay [38], estimating the directivity response of the entire array [39] and identifying the position of the installed microphones [40]. Indeed, small differences between the theoretical and the actual microphone location affect the beamforming result. This is particularly important in the high frequency range (i.e. at 80 kHz, a typical working range in wind tunnel aeroacoustic applications based on airplane models) where an error of few millimeters is comparable to the source wavelength.

The strength of acoustic beamforming is related to the “cooperation” between microphones rather than to the quality of each single sensor, and a calibration procedure that checks the whole array is highly advisable. However, when the count of sensors becomes large, the calibration step could be extremely time consuming. Muller proposed an array calibration procedure [13] based on the reproduction of a white noise monopole source, by means of a small loudspeaker, placed nearby the

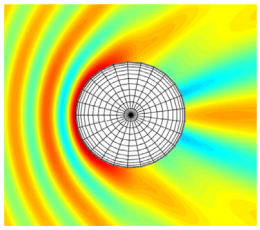

Fig. 3. Planar wave at frequency = 1 kHz scattered on a diffractive solid sphere.

expected source location. The CSM obtained from this measurement step is then used to fully remove systematic differences between microphones and partially correct the effect of sensor positioning errors, at least for sources near to the calibration source.

Finally, it is highly advisable to perform an in-situ calibration [41]. There are at least two main reasons for such final step: it makes it possible to check differences in microphone locations after the final installation of the array (the antenna can indeed undergo damages/deformations that nullify the previous calibration); it takes into account also the test environment and its influence on wave propagation. In wind tunnel applications the in-situ calibration is performed by placing a monopole source inside an anechoic emi-enclosure that avoids reflections so that only the direct path is observed by the array.

3.4. Uncertainty assessment

Acoustic beamforming is a complex measurement system because it is based on the management of a large number of microphones and on an extensive processing of the acoustic signal registered. Consequently, the estimation of the related uncertainty is a complex issue that can be divided into three main aspects:

- source strength estimation;
- source localization accuracy and defocusing;
- sensitivity to ambient conditions, for close environments reflection and diffraction affect the beamforming output.

Reconstruction of the source strength has become very important over the years. The first input to this research field was given by the aeronautic sector, which pushed to find a method to characterize aero-engines acoustic emission. In the 80's, parametric methods were developed based on the assumed knowledge of source locations and the estimation of their strength by a least square error procedure. At the beginning, the method only worked with mutually incoherent sources but Fisher et al. [42] introduced the exploitation of several reference microphones and demonstrated that the restriction based on the assumption of incoherence was excessive. However, the interpretation of beamforming acoustic maps is still challenging because the size and level of the "hot spot" (i.e. the source extension and strength) is influenced not only by the real spatial extent of the source but also by the limited resolution of the array and the loss of coherence in the propagation from the source to the array. Over the years several methods have been developed, ranging from the integration of the acoustic map [13] to more complex approaches based on an eigenvalue classification of microphone cross-spectral matrix [43,44]. However, no definitive solution exists yet and researchers are still tackling this issue by developing methods based on different techniques like those based on deconvolution or on inverse methods. These latter solutions will be discussed in depth in Section 4.

Source localization is widely considered as the main objective in beamforming measurements; this task has been analyzed deeply since the first applications [45], where array localization reliability was only related to the scalar function called the array beam-pattern. In [46] a comprehensive study on the uncertainty of conventional beamforming for 2D linear arrays and far-field propagation was presented. Source location was parametrized in angular terms, in analogy to "vision" systems. Source defocusing issues have also been considered, and an auto–focus procedure proposed. In [47] a multivariate uncertainty analysis targeted to aeroacoustic applications was performed, taking into account also calibration uncertainty. The uncertainty related to sensors selection and microphone phase mismatch was discussed in [48], while the capability of beamforming arrays to reject noise was studied in [49]. In the latter paper, authors demonstrated that, taking advantage from the average effect obtained by using several sensors and from the fact that beamforming exploits a physical wave propagation model, this method considerably attenuates signal components not coherent with the propagation model assumed.

Finally, environmental conditions strongly affect acoustic beamforming reliability; this has been mostly evidenced in aeroacoustic applications and especially in wind tunnel tests. Sound reflection or diffraction induces the presence of ghost sources that occur when the propagation model implemented in the beamforming algorithm does not adequately approximate the real propagation. Beamforming algorithms commonly used in noise source localization tasks are based on a free-field propagation hypothesis, and the propagation model is accurately represented by a Green function. In closed section wind-tunnels [50], this assumption is not valid and the signals acquired, forced to fit to an unrealistic physical model, are mis-interpreted. The main effect is the presence of ghost sources, usually due to propagation paths that include reflections on solid walls, which are not considered in the model. Another typical effect related to the environment is source shift, that is the defocusing and loss in coherence [51] induced by diffraction phenomena which occur when gradients of the sound speed (related to the density, induced by temperature or pressure variation) are present in the propagation medium.

4. Beamforming strategies

This section aims at revising the major research findings in the field of acoustic beamforming that have been issued over the last two decades. The section is structured so as to provide the reader with a path starting from well-established algorithms and then moving on to more complex and application-dependent ones.

4.1. Direct methods

4.1.1. Conventional beamforming

At this point it is worth recalling some concepts. The acoustic pressure measured by a microphone located at $\vec{x}_m$ and due to a source of strength $q$at $\vec{x}_s$ can be expressed as $p_m = qg(\vec{x}_m - \vec{x}_s)$, where $g(\vec{x}_m - \vec{x}_s)$ is the steering vector. In matrix form, and considering M microphones, this can be rearranged as $\mathbf{p} = q\mathbf{g}$. A direct beamformer aims at determining the complex amplitude q at the source location $\vec{x}_s$ by minimizing the expression

$$E = \|\mathbf{p} - q\mathbf{g}\|^2, \tag{13}$$

that leads to a least square solution of the form:

$$\hat{q} = \frac{\mathbf{g}^{\mathrm{H}}\mathbf{p}}{\|\mathbf{g}\|^2}. \tag{14}$$

Eq. (14) can be then rearranged in order to obtain source-auto powers

$$\mathrm{BF}_{\mathrm{cb}} = \frac{\mathbf{g}^{\mathrm{H}}\mathbf{p}}{\|\mathbf{g}\|^2}\left(\frac{\mathbf{g}^{\mathrm{H}}\mathbf{p}}{\|\mathbf{g}\|^2}\right)^{\mathrm{H}} = \frac{\mathbf{g}^{\mathrm{H}}\mathbf{p}\mathbf{p}^{\mathrm{H}}\mathbf{g}}{\|\mathbf{g}\|^4} = \frac{\mathbf{g}^{\mathrm{H}}\mathbf{C}\mathbf{g}}{\|\mathbf{g}\|^4}, \tag{15}$$

where $\mathbf{C}$ is the estimated "Cross Spectral Matrix" (CSM) of the acoustic pressures measured by the microphones. Eq. (15) is also known as *Conventional Beamforming* (CB).

Each steering vector relates the source (either virtual or true)-microphone locations in the propagating medium. This means that each steering vector can be assumed proportional to the columns of the radiation matrix $\mathbf{G}$ describing the acoustic radiation problem $\mathbf{p}_{M\times 1} = \mathbf{G}_{M\times S}\mathbf{q}_S$ in which M microphones and Ssources are considered. Many alternative steering vector formulations are available in the literature [44]. In the simplest formulation, i.e. no-flow and free-field propagation, the element g_{mp} of the steering vector for a generic focus point located at $\vec{x}_p$ and a microphone located at $\vec{x}_m$ can be expressed as:

$$g_{mp} = \frac{1}{|\vec{x}_p - \vec{x}_m|}e^{jk|\vec{x}_p - \vec{x}_m|} \tag{16}$$

In stationary sound fields it is quite natural to exploit averaged auto and cross-spectra. However, exclusion of auto-spectra from the CSM turns out to be actually useful. Indeed, the cancellation of the microphones auto-spectra from the CSM, i.e. the removal of the diagonal term from the CSM, is beneficial because these data contain self-noise from the individual channels, e.g. wind noise, electronic noise, that does not cancel out as it does in the out-of-diagonal terms (since self-noise between different channels is supposed to be incoherent). Moreover, the microphone auto-spectra do not contain any phase information, therefore they are of no aid in the beamforming process. The "trimmed" CSM is built so that

$$C_{mm'} = \begin{cases} 0 & \text{if} m = m' \\ \langle P_m P^*_{m'} \rangle & \text{if} m \neq m' \end{cases} \tag{17}$$

for $m, m' = 1 \ldots M$. In Eq. (17) the term $\langle\cdot\rangle$ stands for the averaging operator.

4.1.2. Adaptive beamforming

The term *Adaptive beamforming* includes different techniques that aim at optimizing some processing variables, such as the weight pattern or phasing of the microphone array, in order to improve performance parameters like resolution, MSL, etc. Adaptive beamforming algorithms therefore seek to reduce or nullify signals coming from directions different from the focus one. Moreover, the adaptive process is constrained to maintain a predetermined sensitivity in the focus direction, thus a signal arriving in the focus direction is not canceled. One of the first examples of adaptive beamforming for radar applications was presented by Howells [52]. Howells introduced the so-called intermediate frequency Side Lobe Canceller (SLC), in which interfering noise was canceled by exploiting auxiliary sensors and properly mixing the signals received by both the radar and the auxiliary antenna. The method was then further developed by Applebaum [53], who presented an approach to adaptively maximize the beamforming output SNR. Both approaches exploited a D&S beamformer to provide the primary input and further sensors to provide the reference input.

Over the years several methods have been developed and presented to the scientific community, such as the Windrow-Hoff *Least Mean Square* (LMS) algorithm [54], the Capon Minimum Variance Distortionless Response (MVDR) [8], and the Reed algorithm [55], a fast convergence method also known as the *Sample Matrix Inversion* (SMI). The latter approach faced the major drawback of adaptive algorithms, the rate of convergence. Indeed, sometimes this rate is too slow for practical applications. In [56] a constrained least-square algorithm, also known as the *Linearly Constrained Minimum Variance* (LCMV) beamforming, was developed to optimize the array performance in real-time. The adaptation was performed iteratively, by modifying sensor weights to minimize noise power [57]. Research on overcoming the limitations of the aforementioned methods is still active. To cite some research works, Stoica et al. [58] and Li et al. [59,60] proposed a robust implementation of the Capon beamformer which extends the MVDR approach in case of uncertain steering vectors; Jung et al. [61] developed

a Generalized Eigenspace-based Beamformer (GEIB) which utilizes the eigenstructure of the correlation matrix to enhance the performance of the LCMV beamformer. Other applications of adaptive beamforming methods can be found in the work by Dmochowski et al. [62], in which a spatiotemporal framework for spectral estimation based on the LCMV method was proposed, to reduce contribution from unwanted noise and reverberation on the target signal.

All mentioned methods are not inherently adaptive, since they can be used also in an off-line setup. Moreover, even though they have been initially developed for signal extraction, they are exploited for noise source localization when fast computational requirements with high number of microphones drive the application, see for instance [63]. The recent interest in adaptive beamforming algorithms has been demonstrated by the work of Dougherty in [64], who proposed another formulation of the Capon beamforming that should ease the exploitation of the method for those working in noise source localization.

4.1.3. Orthogonal beamforming

Orthogonal beamforming was proposed by Sarradj in [65], starting from the observation that many acoustic phenomena encountered in practice are linked to different source mechanisms (e.g. aerodynamic, thermal or mechanical ones), which may result in different sources. If these sources are assumed to be temporally and spatially uncorrelated, they can be considered orthogonal and therefore the sound field can be approximated by a summation of these orthogonal components. This results in a pressure measured by the m^{th} microphone which can be modeled as $p_m = \sum_{j=1}^{J} f_{mj} q_j$, where the f_{mj} factors depend on the source-microphone location. This orthogonality condition causes the cross spectral matrix to be rewritten as $C_{mm'} = \sum_{j=1}^{J} C_{mm',j}$, thus allowing to map each j^{th} source mechanism separately if the term $C_{mm',j}$ replaces the term $C_{mm'}$ in Eq. (15). Sarradj suggested calculating each orthogonal component by exploiting the eigenvalue decomposition of the cross-spectral matrix, it being Hermitian and positive semidefinite. Indeed, the eigenvectors are orthogonal while the eigenvalues, which are positive and real-valued, approximate the source strengths. In this way the $C_{mm',j}$ term can be expressed as $C_{mm',j} = \mathbf{v}_j \lambda_j \mathbf{v}_j^H$. The full mathematical derivation of the method can be found in [44], while a further application to a cleaning vehicle is described in [66].

4.1.4. Functional beamforming

Functional Beamforming (FB) was introduced by Dougherty in [67]. It deserves attention because, despite being quite simple in nature, it increases flexibility in array design and improves the dynamic range. Functional beamforming takes its name from the exploitation of functions of matrices in the algorithm. The rationale of the method consists in raising the CSM to the power of the reciprocal of a parameter v in the functional sense, as

$$\mathbf{BF_{fb}} = \left(\mathbf{g}^{\mathrm{H}} \mathbf{C}^{\frac{1}{v}} \mathbf{g}\right)^{v}. \tag{18}$$

The overall raising to power of v is needed for a correct estimation of source strength. Computation time of FB does not exceed that of CB, since the only addition is the effort to perform a spectral decomposition of the CSM. Common values for v range from 20 to 300. It is interesting to notice that for $v = 1$ FB reduces to CB, while for $v = -1$ it produces the MVDR beamformer. In any case, it is natural to set $v \geqslant 1$ to get significant sidelobes attenuation and to improve resolution. The major advantage of FB holds if the steering vectors are accurately set: this requires an accurate calibration, the use of a correct physical model for $\mathbf{g}$ and a properly set calculation grid.

There have been several applications of FB over the last years. An application on landing aircraft flyovers can be found in [68]. It was shown that the FB approach can make it possible to test aircrafts under operational conditions at a relatively large observer-aircraft distance using an array of only 32 microphones. An improvement of the dynamic range of about 30 times and of the spatial resolution of about 6 times was reached with respect to CB. In [69] functional beamforming was exploited in an interior acoustic application, i.e. source localization inside a cabin. A rigid spherical array was utilized by for the purpose. Yang demonstrated that quantification error increases when the real source is not "focused" (i.e. the distance from the array to the source is not accurately known) or the focus direction is wrong, and suggested solutions to overcome this issue.

4.1.5. Combined array methods

This section addresses all those beamforming approaches which combine either different areas of the same microphone array or different microphone arrays to enhance the source localization task. The former concept was proposed by Guidati and Sottek in [70]; they presented a modular microphone array whose geometry could be adjusted so as to tweak the array aperture to the acoustic test as well as to combine the results of the different antennas thus obtained. Elias [24] introduced what he called *multiplicative beamforming* to enhance the poor performance of cross-shaped arrays with conventional beamforming. He suggested to retain from the array cross spectral density matrix only those cross-terms that relate the two arms of the array. This choice makes it possible to exploit shading techniques and obtain better performance in terms of source localization. This approach was also tested in flyover applications [71,72]. Indeed, the multiplicative approach was already known to the community of those working on underwater acoustic [73], although it had been introduced in a different way from the one presented by Elias. The multiplicative approach, which consisted in multiplying the beamformer output of different arrays, was also recently discussed for aeroacoustic dipole source localization problems by Porteous et al. in [74].

A similar concept, though exploited for applications in interior noise source localization, was presented in [75,76]. The solution identified in these papers exploited a double-spherical array: the inner part is a rigid array, well suited for the mid-high frequency range, while the outer part consists of an open spherical array targeted to extend the frequency range to low frequencies. The combination of the two antennas takes place in the mid frequency range (500–1500 Hz) exploiting a patented coherence processing between partial beamforming outputs so as to keep true sources while rejecting ghost sources due to their spatial un-coherent properties. The mid frequency range is the only one in which this processing can be exploited because in this range the inner array has good directivity but poor resolution and the outer array has good resolution but poor directivity, and therefore both the arrays are simultaneously exploitable.

Another solution exploiting the combination of multiple beamformer outputs, even though related to the same array, was proposed by Castellini in [77]. His approach, which he called *Averaging Beamforming* (AB), was based on a statistical analysis of the beamformer outputs collected by placing the microphone array in different positions inside the testing environment. The rationale of this strategy comes from the observation that "true" noise sources, i.e. those not related to reflections nor sidelobes, are localized in the same position with respect to the global reference system, regardless the location of the microphone array with respect to the same reference system. On the other hand, when the array is placed in different positions, pseudo-sources move along, due to different reflection paths and to the different locations of array sidelobes. By repeating measurements from different locations, it is possible to obtain a data set that can be processed in a statistical sense, i.e. by estimating the average and sample standard deviations of the beamforming outputs. Thus, it is possible to recognize pseudo-sources (e.g. reflections or sidelobes) and remove them. The main drawbacks of AB are the need of a stationary sound field and the sensitivity to source directivity. Indeed, without a stationary sound field the antenna would measure different acoustic pressures whenever its position is changed, while if a source is too directive, e.g. as it can be the case in high frequency emissions, in some positions it might have different strength.

4.2. Deconvolution methods

Deconvolution methods have raised interest in the acoustic array community for giving the possibility to improve the resolution of the array and reduce the unwanted side-effects of side-lobes. These methods, though already known in astronomy and other fields, like the CLEAN algorithm introduced by Jan Hogbom [78] for astronomy and further applied to geosciences for rain rate analysis [79], did not immediately catch on in the acoustic field, mainly because of the computational burden required compared to classical beamforming approaches. However, with the increase in computational power of computer processors, they have started to be investigated more in-depth by acousticians. Nowadays, it is quite common to hear about deconvolution methods, however a clarification is still required in a beamforming review. Every beamforming map can be considered a "dirty map" $b(x,y)$ because it is spoiled by the presence of side-lobes and because of the influence of the array geometry, which can distort the acoustic image just like a lens can in an optical application. Just as in optics it is possible to compensate for lens distortions, also in array acoustic it is possible to reduce the influence of the array by assuming that the dirty map is nothing more than the convolution of a certain source distribution $q(x_s,y_s)$ and the point spread function $p_s(x,y|x_s,y_s)$ (3.1) relating the positions of observer (x,y) and source (x_s,y_s)

$$b(x,y) = \sum_{(x_s,y_s)} q(x_s,y_s)p_s(x,y|x_s,y_s). \tag{19}$$

The aim of deconvolution methods is therefore to find a source distribution fulfilling Eq. (19) under the constraint $q(x_s,y_s) > 0$. This given, it should result clearer that this mathematical problem can be solved in several ways, and this explains the number of algorithms proposed by researchers to accomplish this task.

One of the first examples is represented by Dougherty and Stoker [80], who first utilized CLEAN in array acoustic measurements. CLEAN is based on the iteratively cancellation of PSFs peak sources from the original "dirty map" in order to obtain the "clean map". This deconvolution method proved to be a promising approach, but it is limited by the fact that it is related to synthetic PSFs, which are frequently different to the true beam pattern of dominant sources. Indeed, this technique is powerful when the acoustic field can be modeled as the superimposition of point sources, but suffers in case of:

- multiple incoherent sources
- non–point sources, e.g. slotted trailing edge
- source with non-uniform directivity
- presence of non-uniform flow or when the flow Mach–number (i.e. ratio between flow speed to the local speed of sound) is inaccurately estimated
- inaccurate microphone calibration.

To overcome the above mentioned problems the CLEAN–SC algorithm was developed by Sijtsma [81,82]. The algorithm is based on Source Coherence (SC), and it has become one of the most popular and widely recognized processing method for mapping enhancement, as testified by the active work on its improvement [83,84]. CLEAN-SC does not use synthetic PSFs, but is based on the evidence that side-lobes are spatially coherent with their main sources. CLEAN-SC therefore iteratively removes the part of the acoustic map which is spatially coherent with the main source, making it possible to enhance both

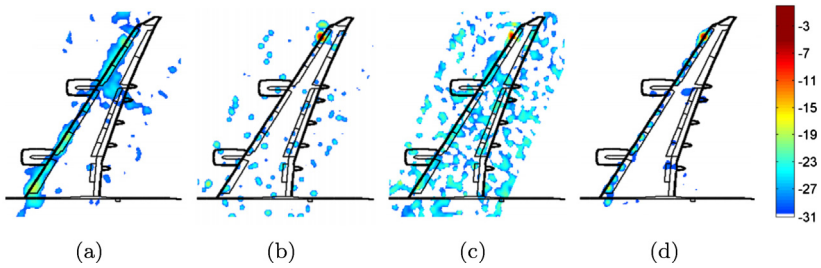

Fig. 4. Acoustic source map (source power normalized to the highest peak level - dynamic range: −31 dB) obtained from CB after coherent source removal (*a*), DAMAS (*b*), CLEAN PSF (*c*), CLEAN SC (*d*) [82] at 12360 Hz.

spatial resolution and dynamic range, unmasking secondary sources. It should be pointed out that sometimes CLEAN-SC is not recognized as a "true" deconvolution method, because it does not make use of any PSFs. However, this approach must be listed among the deconvolution methods because it fully fulfills the aim of deconvolution approaches, i.e. finding a source distribution that improves beamforming resolution and reduces side-lobes. Moreover, one of the advantages of CLEAN-SC is that its computational demand is almost equal to that of conventional beamforming. One of the widely recognized deconvolution methods is the DAMAS (Deconvolution Approach for the Mapping of Acoustic Sources) algorithm proposed by Brooks and Humphreys in 2004 [85]. This is an iterative deconvolution method which tries to look for an exact solution of the matrix form of Eq. (19) by a Gauss-Seidel type relaxation. The computational burden of DAMAS is quite high, and for this reason it has not become a breakthrough in beamforming algorithms. However, the pioneering work by Brooks and Humpreys, triggered the activity of the acoustic community on deconvolution methods and further evolutions of DAMAS have been presented over the years, starting from the DAMAS-C [86], DAMAS2 and DAMAS3 [87,88] and continuing with the approaches described in [89,90]. In [91] a time domain Adaptive Noise Cancellation (ANC) algorithm was combined with DAMAS for background noise reduction and applied for the processing of acoustic pressure measured by an out-of-flow microphone array in an open-jet wind tunnel where typical SNRs are as low as −29 dB. As already pointed out, there are several ways to solve the problem of Eq. (19). Some that deserve to be cited are the Non Negative Least Square approaches (NNLS, FFT-NNLS) [92], the deconvolution methods based on the Richardson-Lucy (RL) algorithm [93–95]. The interested reader might also refer to the works of Ehrenfried and Koop [96] and Chu [97] for a comparison of these different deconvolution approaches, also in terms of computational sustainability. Other approaches worth mentioning are the LORE (Localization and Optimization of Array REsults) approach [98], which tries to recognize patterns inside a CB map and relates them to a noise source distribution that would produce the same map, and the algorithm presented by Bahr [99], which is based on a wavespace transformation of the array data. The wavespace method exploits Fourier transforms to quickly evaluate a shift-invariant convolution and make it possible to determine the magnitude and relative phase of multiple coherent sources. Computational effort is also analyzed by Bahr [99], who proposed an interesting multiscale approach to accelerate solution convergence.

To give the reader a visual idea of the effect of deconvolution methods on a BF map, some results reporting the acoustic images obtained with the most common deconvolution methods are illustrated hereafter in Fig. 4.

4.3. Inverse methods

The direct radiation problem described in Section 4.1.1 represents the starting point of any acoustic localization problem. However, even though sharing the same initial formulation, direct and inverse methods approach the problem in a completely different way. Indeed, direct methods solve a *scalar* problem in the sense that each source is resolved separately from the others and the beamformer is scanned over certain "focus areas" until the potential source locations are identified. An implicit assumption that sources are uncorrelated among each other is therefore made. On the contrary, inverse methods aim at tackling the problem for all sources at once, i.e. they aim at finding the best source distribution which can optimally approximate the pressure distribution at the microphone location. Since source interference is thus potentially taken into account, inverse methods can deal with correlated/uncorrelated and sparse/spatially-distributed sources. This key concept explains the increasing interest in this approach over the years, even though different communities have addressed the problem, giving rise to a non-unified naming structure. The main cause of such a wide bunch of techniques is related to the choice of the source nature used in the formulation of the problem, ranging from the plane wave formulation of NAH [100] and SONAH [101,102], the spherical wave expansion of the HELS method [103,104] to the IBEM [105,106] and Equivalent Source Method (ESM) [107–109] formulation, which uses functions obtained by adopting the Boundary Element Method to address the radiation problem.

The name "inverse methods", though being more general, addresses the acoustic problem better than the term "inverse beamforming", which, however, is more familiar to the beamforming community, since "no beams are formed" and no scanning over focus points is performed. In fact, in inverse methods the surface of the physical source is virtually covered with a

cloud of elementary sources (e.g. monopoles, dipoles or multi-poles); the spatial and strength distribution of these sources is estimated by solving the inverse radiation problem described in

$$\hat{\mathbf{q}} = \mathbf{H}\mathbf{p}. \tag{20}$$

where $\mathbf{H}$ represents an inverse operator. Indeed, this operator can assume different forms, depending on the solution strategy adopted. A complete review about different inverse operators is provided by Leclère et al. in [110]. When the acoustic field is stationary, the former problem can be rearranged in terms of Auto- and Cross- Power Spectra averaged over several observations:

$$\mathbf{G}\mathbf{Q}\mathbf{G}^H = \mathbf{P}. \tag{21}$$

The matrix $\mathbf{P} = \langle \mathbf{p}\mathbf{p}^H \rangle$ is the Cross Spectral Matrix – CSM – of pressure at microphone locations and $\mathbf{Q} = \langle \mathbf{q}\mathbf{q}^H \rangle$ is the CSM of sources strengths ($\langle \cdot \rangle$ is the average operator). Using the quadratic form, the solution of the inverse problem can be obtained as

$$\hat{\mathbf{Q}} = \mathbf{H}\mathbf{P}\mathbf{H}^H. \tag{22}$$

Solution to the quadratic form can be obtained, for instance, exploiting the *Covariance Matrix Fitting* (CMF) [111,112] approach, that means solving the quadratic form of acoustic problem in order to find the combination of sources that produces the "best" fitting of the measured CSM. An assumption of uncorrelated sources is made this causing the source power matrix $\mathbf{Q}$ to become diagonal. This allows to easily rearrange the quadratic form as a standard linear system and force a real solution.

Since the number of unknowns S, i.e. the source strengths, is typically much greater than the number of known variables M, i.e. the pressure data at the microphone locations, the problem is generally under determined [113]. Moreover, the problem is also ill-posed in Hadamard sense [114]. The reason is twofold: the solution can be non-unique, because the system is typically under-determined, and the solution highly depends on the problem data, i.e. noise on measured data or uncertainty on propagation model may lead to heavily perturbed solutions. For all these reasons, it is common practice to find the minimum-norm solution of the problem addressed in Eq. 20 by either exploiting the Moore–Penrose pseudoinverse (as $S > M$ the right-inverse is used) or regularization strategies like the Tikhonov approach [115]. Weighting strategies, in which a pre-conditioning matrix (typically is a square diagonal matrix of size $S \times S$, with non-zero real elements on the main diagonal) is used in the general Tikhonov formulation, can also be adopted. These approaches aim to either introduce a priori information about the sources, as suggested by Padois et al. [116], who exploit a Conventional Beamforming map as weighting matrix, or to balance the energy required by sources acting at different distances with respect to the sphere, to generate the same pressure at the array centre, as proposed by Pereira in [117,118]. An in-depth analysis of the regularization principle to use is out of the scope of the present paper, but the reader should be aware of this issue when approaching an inverse formulation in a source localization problem.

Acoustic imaging techniques based on inverse methods carry several advantages with respect to direct beamforming approaches. Apart from the higher dynamic range and better resolution, the most important advantage is that they provide quantitative results of the source strength. Indeed, while direct methods can give this estimation as if the source at a certain focus point is the only one acting (even though some integration methods can be adopted once the acoustic map is produced [13]), inverse approaches take into account all sources at once, therefore a more accurate strength evaluation can be performed. This is true as long as proper a priori information of the sources is given [110], e.g. a sparsity condition is respected (the source distribution is modeled by few non-zero components). Sparsity can be enforced by reformulating the problem in terms of L_p-norm

$$\hat{\mathbf{q}}(\lambda, p) = \arg\min_{\mathbf{q}} \left(\|\mathbf{G}\mathbf{q} - \mathbf{p}\|_2^2 + \lambda^2 \|\mathbf{q}\|_p^p \right) \tag{23}$$

and minimizing for $p < 2$. A value of $0 \leqslant p \leq 1$ enforces sparsity in severe under-determined problems (e.g. volumetric mapping), even though for $p < 1$ this results in a non-convex optimization problem. The L_0-norm minimization can be approximated by the *Orthogonal Matching Pursuit* [119,120] algorithm. This is a greedy algorithm that selects only those sources which give the best approximation of measured data. A version of the algorithm making use of cross-validation principle [121] reduces possible reconstruction errors. The L_1-norm minimization can be calculated by means of *Least Angle Regression Lasso* algorithm [122].

Iterative inverse methods are a family of methods which can cope with this requirement. An example of this is represented by the Generalized Inverse Beamforming (GIBF) presented by Suzuki in [123]. At each iteration the number of equivalent sources is reduced according to a source strength-based criterion, thus enforcing sparsity and reducing numerical issues. GIBF was later improved by Zavala et al. [124,125] in order to calculate also the strength of correlated sources. They introduced an automated regularization factor to be estimated at each iteration of the calculation procedure. Presezniak et al. [126] presented a weighting matrix approach that aimed at increasing the dynamic range of GIBF, thus making it possible to resolve more closely spaced sources. The weighting matrix, whose elements are obtained by a dedicated optimization procedure, right-multiplies the propagating function $\mathbf{G}$(before the inversion), thus putting more emphasis on certain locations with respect to others. Colangeli et al. performed a dedicated analysis to identify the best regularization strategy to be

adopted with GIBF [127]. They demonstrated that the most effective regularization method is based on the Tikhonov approach when combined with the quasi-optimality function to extract the regularization parameter. An interesting formulation of GIBF for the assessment of jet noise was given by Dougherty in [128]. He proposed to recast the radiation equations in order to solve a generalized direct problem. The *Iteratively Reweighted Least Squares* - IRLS - [129,130] algorithm can be used for obtaining sparse solution.

To tackle the inverse radiation problem, Antoni [131] proposed a different approach that exploits Bayesian inference. This method relies on the observation that the inverse problem of Eq. (20) can be reformulated in terms of weighted spatial basis expansion ϕ_k:

$$\hat{\mathbf{q}} = \sum_{k=1}^{P} c_k \phi_k, \tag{24}$$

where c_k represents coefficients which depend on the pressure data measured $\mathbf{p}$ and the spatial functions, ϕ_k, are independent from the measured data but strongly related to the topology of the calculation point distribution and the geometry of the array. Antoni proposed to view the coefficients as random variables that produce a random source field (in the sense of the experimenter's residual lack of knowledge on the field) and look for its probability distribution $[q(\mathbf{c}, \boldsymbol{\phi})|\mathbf{p}]$ given the measured data $\mathbf{p}$. He demonstrated that the optimal basis functions are the *M*-eigen functions of a specific continuous-discrete propagator linked to prior spatial information about source distribution and measurement noise. This approach holds several benefits like an implicit regularization mechanism and has higher resolution capabilities with respect to other methods (the so-called *Bayesian focusing*). In [132] a comparison between the Bayesian formulation and classical Equivalent Source Method (ESM) formulation exploiting different regularization strategies is discussed. Pereira et al. showed that this classical formulation can be obtained as a particular case of the Bayesian one. An evolution of the work was lately presented by Pereira et al. in [133], in which they propose a method, based on Bayesian formulation, to automatically select a good regularization parameter when solving inverse problems in acoustics.

Another approach worth mentioning is the one proposed by Castellini et al. in [134]. Their aim was to demonstrate the possibility of retrieving phase information, which is commonly lost in standard approaches, from a beamforming processing. Castellini et al. proposed to exploit an iterative optimization algorithm based on monopole source substitution after the calculation of a beamforming map (see Fig. 5). The optimization strategy makes it possible to avoid the inversion of the propagation matrix.

4.4. Spherical harmonics decomposition methods

When dealing with spherical microphone arrays it is a quite common solution to decompose the sound field into orthogonal basis functions called *Spherical Harmonics* (SHs) [37]: this approach is addressed as *Eigenbeamforming* or *Spherical Harmonic Beamforming* (SHB), even though the latter is specific for spherical waves. It is out of the scope of this paper to provide an in-depth theoretical discussion about Spherical Harmonics Decomposition (SHD), for which the interested reader can refer to [135], however, it is indeed worth recalling briefly some concepts. A monopole source located, in spherical coordinates with respect to the center of a sphere of radius *a*, at (r_0, θ_0, ϕ_0), will produce a pressure on a point of that sphere which can be expressed as

$$p(k, a, \theta, \phi) = \sum_{n=0}^{\infty} R_n(ka, kr_0) \sum_{m=-n}^{n} Y_n^m(\theta_0, \phi_0)^* Y_n^m(\theta, \phi). \tag{25}$$

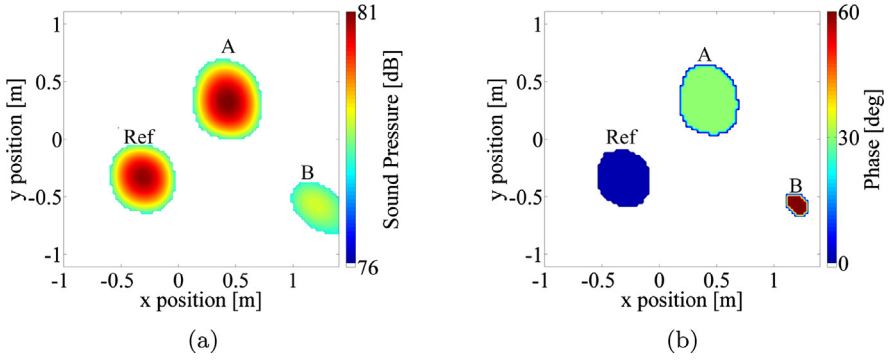

Fig. 5. Amplitude (a) and phase (b) maps of a three monopoles sound field at 1000 Hz from [134].

In Eq. (25) the term $Y_n^m(\theta,\phi)$ addresses the Spherical Harmonics, which, combined together in the inner summation, drive the angular behavior of the expansion, while $R_n(ka,kr_0)$ is the term that drives the radial amplitude. By changing the definition of $R_n(ka,kr_0)$, the pressure distribution for an incident wave can be estimated taking into account both the source type (plane *vs.* spherical) and the acoustic transparency of the sphere (hard *vs.* transparent). Eq. (25) can be rewritten exploiting the Spherical Fourier Transform (SFT) [135] as

$$p(k,a,\theta,\phi)=\sum_{n=0}^{\infty}\sum_{m=-n}^{n}C_n^m Y_n^m(\theta,\phi) \tag{26}$$

where C_n^m represent the coefficients of the SFT of the pressure $p(k,a,\theta,\phi)$. By comparing Eq. (25) and (26), it is clear that $C_n^m = R_n Y_n^m(\theta_0,\phi_0)^*$; this leads to the following ideal beamformer formulation

$$\mathrm{BF}_{\mathrm{SHB}_{\mathrm{ideal}}}(\theta,\phi,\theta_0,\phi_0)=\sum_{n=0}^{\infty}\sum_{m=-n}^{n}\frac{C_n^m}{R_n(ka,kr_0)}Y_n^m(\theta,\phi), \tag{27}$$

which results in a sharp peak pointing towards the source with no sidelobes. The real scenario is different from this ideal formulation for two reasons: the source model can differ from the monopole assumption and the pressure field is not known over the entire sphere, since the pressure field is sampled only at *M*discrete locations. The latter aspect causes the SFT to be discrete and, therefore, the Fourier coefficients become an approximation $\widetilde{C}_m^n$ of C_m^n. This implies that the first summation has to be truncated up to a certain order *N*which guarantees that the Fourier coefficients are correct and the Spherical Harmonics are orthogonal [136]. As a general rule, the order N must be chosen so that $M>(N+1)^2$ and $N\approx(ka+1)$. Taking into account all these aspects, Eq. (27) can, therefore, be rewritten as

$$\mathrm{BF}_{\mathrm{SHB}}(\theta,\phi,\theta_0,\phi_0)=\sum_{n=0}^{N}\sum_{m=-n}^{n}\frac{\widetilde{C}_n^m}{R_n(ka,kr_0)}Y_n^m(\theta,\phi). \tag{28}$$

It should also be recalled that the accuracy of the Fourier coefficients up to order N is ensured by the introduction of an integration weighting factor, α_i, associated to each i^{th} microphone. Depending on the spatial distribution of the sampling points these weighting factors can be constant or not. It is then clear that spatial sampling over the sphere represents a fundamental aspect. In fact, to guarantee the shift–invariance of the beam pattern, the orthogonality of the Spherical Harmonics needs to be ensured. This is not a trivial task and several sampling distributions have been proposed over the years. The interested reader can refer to [135] for a complete overview of those methods.

The scientific community has been very active on SHD-based methods since the early 2000. The first application for acoustic source localization was presented in [137], where a circular microphone array mounted on spherically shaped objects was used to perform beamforming. The general concept of phase modes was discussed and beam patterns were generated taking into account diffraction caused by the sphere. With a 16-element circular array located at the equator of a sphere (diameter of 0.17 m), very good performances in terms of gain and directivity were obtained also in the low frequency range (from 300 Hz to 5 kHz). This activity set the foundation for the research activity on spherical arrays, as testified by the work of Meyer and Elko in [138], which triggered the evolution of eigenbeamforming [139] for spherical arrays. Rafaely published several papers on this subject in the same years. In [140] he reported a very interesting discussion about spatial resolution and computational efficiency of the plane-wave decomposition of the sound pressure on a sphere, while in [141] he compared different layouts of microphones distributed over a spherical surface. That paper provides a useful guide for spherical microphone array design and reports a performance analysis which takes into account the number of sensors, their positioning accuracy and how measurement noise can affect beamforming results. Rafaely [142] also performed a comparison between D&S and SHD beamforming. He showed that the performance of the two solutions differs mainly in the low frequency range, where the SHDs-based processing, because of its intrinsic combined spatial filtering/data fitting action, makes it possible to have a constant directivity with no deteriorations. The performances in the high-frequency range are typically limited by aliasing, i.e. high-order spherical harmonic coefficients are aliased into lower orders, as analyzed in-depth in [143]. In this paper Rafaely et al. also introduced spatial anti-aliasing filters and discussed how these filters can reduce the spoiling effects of aliasing on the beampattern. A flexible method to cope with microphone positioning uncertainty in real-world systems was presented by Li and Duraiswami in [144]. They proposed an iterative adaptive implementation based on a White Noise Gain (WNG – i.e. the ratio of the SNR at the array output to the SNR at each single microphone subjected to spatially uncorrelated white noise – the higher the WNG, the more robust the array) [145] constrained optimization which makes it possible to calculate the vector of the complex weights to be assigned to each microphone of the array and, therefore, converge to the desired beamformer of a specified order in any steering directions. Later Haddad and Hald in [146] introduced a scale factor to correct the pressure distribution spoiled by the scattering of the hard sphere; they called this approach Spherical Harmonics Angularly Resolved Pressure (SHARP). In [147] Hald also presented an improvement of the same method based on the introduction of a set of Finite Impulse Response (FIR) filters optimized to minimize the highest sidelobe in a Filter And Sum (FAS) beamformer thus guaranteeing better sidelobe suppression and, therefore, a higher dynamic range. The computational burden linked to the evaluation of these optimal filters, different for each focus point, was tackled by pre-calculating them for a pre-defined calculation mesh and by storing them in a database, in order to solve

the filter coefficients calculation for an arbitrary point in the space as an interpolation between the filter vectors associated to a set of neighboring points. An interesting approach to improve the performance of a spherical array at low frequency, where spheres of bigger diameter should theoretically be exploited, was proposed By Tiana-Roig et al. in [148]. They suggested to perform SHB on virtual pressure data calculated by acoustic holography from a physical hard spherical array, at a larger diameter with respect to the original sphere. They demonstrated that this approach produces better resolution to the detriment of a lower MSL, which is sensitive to noise. A quite recent work worth citing is the one of Chu et al. [149]. They suggested to adapt deconvolution approaches as DAMAS, NNLS, RL and CLEAN to SHB in order to improve spatial resolution and achieve wide dynamic range. Very recently, Battista et al. [150] proposed to use SHD to spatially filter the complex pressure distribution (thus filtering out the noise contribution at higher spatial frequencies) in order to stabilize the inverse acoustic problem faced in the GIBF formulation. They demonstrated that, when the source-receiver propagation model is appropriate to describe the acoustic environment in which the test takes place and noise is not spoiling excessively measurement data, the SHD approach is sufficient to obtain a regularized solution. If these conditions are not satisfied, SHD can enhance GIBF results when used as a pre-processing step in a twofold procedure involving classic Tikhonov regularization.

4.5. Three-dimensional beamforming

Beamforming results are typically presented as 2D planar acoustic images. Indeed, this representation is very useful for assessing the performance of new algorithms, because it gives the reader an immediate impression of the potentials of the methods. However, especially in the last years, there has been an increased trend in exploring the possibility of calculating beamforming results on a 3D space, the latter being either a three-dimensional surface enveloping the system under analysis or a volume so as to provide a "tomographic-like" visualization of the source.

The 3D representation is typical of interior beamforming applications, as it will be discussed in Section 5.3. It is also quite common to choose this strategy when analyzing complex shaped systems as the envelope surface of a car body or of an airplane fuselage with multi-arrays. An example of the latter application can be found in [151] and in [152]. In particular, Doebler et al. suggested computing a beamforming map for each one of the three arrays (5 m $\times$ 3 m array, each equipped with 192 electret microphones) and merging the resulting maps onto a 3D surface enveloping the Porsche "Panamera S" body, taking into account proper weightings dependent on the visibility of the car from each array. Pressure amplitudes were also normalized by comparing the medians of the sound pressure levels of the points visible to every array. They also showed CLEAN-SC to be an efficient deconvolution method for that particular application.

There are very few works aiming at providing a "volumetric" representation of the source [153–158,74]. This is the "true" three-dimensional (3D) beamforming. In [153] Brooks and Humprheys proposed the exploitation of the DAMAS approach to target 3D applications. They started investigating several arrays of different size and design and their beamforming capability to focus longitudinally and laterally, demonstrating that large arrays with microphones concentrated towards the center are advantageous for the purpose. The important result provided in [153], obtained by considering different sources at different frequencies, is that, for the design investigated, the longitudinal beamwidths are large compared to the lateral beamwidths, nevertheless DAMAS can still be used to extract source location and strength. Dougherty [154] compared the performances of CLEAN-SC, DAMAS, TIDY and eigenvalue cancellation to cage array data for a 3D localization of turbofan engine jet noise sources. He performed this analysis by calculating beamforming on 19600 points, equally distributed on 16 transverse planes separated by 0.5 m, demonstrating the feasibility of imaging the structure of the shear layer noise, even though each technique provided different source locations. Xenaki et al. [159] proposed two Fourier based deconvolution approaches (the first one based on a transformation of coordinates trying to make the point spread function more shift invariant, the second one combining the transformation of coordinates with an alternative scanning technique) to improve the quality of three-dimensional beamforming with phased-arrays. Legg and Bradley [155] compared the amplitude and localization accuracy given by CLEAN-SC for 2D and 3D scanning surfaces when exploiting a spherical array. They proved that 3D scanning surface provides higher localization accuracy for higher frequencies and for sound sources located close to the array. Sarradj, who has been active in the analysis of 3D beamforming, pointed out that, even though the extension to 3D is straightforward in principle, a deconvolution approach is mandatory [157]. A first insight into the superiority of 3D beamforming in enhancing noise source distribution with respect to standard 2D mapping was presented in [156], where an application to airfoil leading edge noise source localization was described (see Fig. 6). In [158] Sarradj compared four dif-

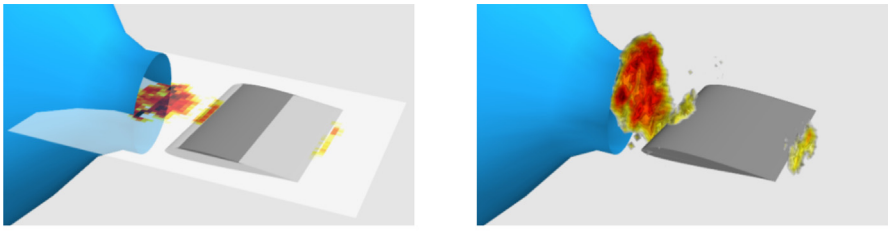

(a) (b)

Fig. 6. CLEAN beamforming 2-D *(a)* and 3-D *(b)* mapping (6.3 kHz, 35 dB dynamics) [156,157].

ferent formulations of the steering vector to be used in 3D beamforming applications. He pointed out that two formulations provided higher localization accuracy to the detriment of a worse source level estimation. However, he also pointed out that, since in a 3D application the high number of calculation points demands for a computationally efficient deconvolution technique like CLEAN-SC, localization accuracy becomes the key aspect to be taken into account. Another work worth citing is the one by Porteous et al. [74], in which the performances of four beamforming algorithms (namely conventional cross-spectral beamforming, conventional beamforming coupled with CLEAN-SC, ‘‘multiplicative”-cross-spectral beamforming and ’multiplicative’ beamforming with CLEAN-SC) for the localization of acoustic dipole sources in a 3D domain (used to represent sound sources generated by flow-body interaction) were compared. With respect to the previous works cited, Porteous et al. used two arrays placed orthogonally to each other to exploit the multiplicative approach. A similar work worth citing is the one by Padois and Berry [160], in which they compare several microphone array techniques (Clean-SC, L1-GIBF, DAMAS and SC-DAMAS) in the case of two and three-dimensional scan zones. Ning et al. [161] proposed the use of Compressive Sensing in three-dimensional imaging with planar arrays. Very recently, Battista et al. [162] investigated different solution strategies to the inverse acoustic problem (ESM-IRLS, CMF-OMPCV, CMF-LassoLars, CMF-IRLS) for mapping volumes of potential noise sources rather than surfaces in case a single planar array is used in aeroacoustic applications.

4.6. Enhanced time-domain methods

If it is true that the first beamforming algorithm was developed in the time domain using simple analogue delay lines, it is also true that the major step forward in this field have been performed thanks to the progress in digital signal processors by working in the frequency domain. However, an increased interest in time-domain algorithms has been registered over the years. The reason is twofold: time-domain approaches are more suitable for the analyzes of acoustic problems involving time-varying sources; a beamforming algorithm providing a time history as an output opens the way to a bunch of applications, like machine diagnostics and sound auralization, that are of great appeal for industrial end users. The interest in time-domain beamforming has also been supported by the increased performance of computers and computational strategies (e.g. GPU computing [163]).

An interesting paper to be cited is the work of Jaeckel [164], in which the author made a balance of the pros and cons of time and frequency domain approaches, with a particular focus on time-domain strategies. In [165] Dougherty proposed a time-domain approach implementing diagonal deletion on a cross array to mitigate microphone self-noise.

In [166] a High-Dynamic-Range time domain beamforming algorithm providing automatic and iterative decomposition of the sound field is presented. It is a sort of CLEAN algorithm, but in the time domain, and allows a contrast improvements up to 50 dB.

Very recently Quaegebeur et al. [167] presented an alternative formulation of time-domain beamforming which exploits the combined use of generalized cross-correlation and spatial weighting functions that take into account the relative microphone-focus point location. They demonstrated that the method is computationally efficient and provides an increase in accuracy. In [168,169] beamforming is used to localize impulsive sound sources. While the wide-band spectrum of impulses shade the map in the frequency-domain, time-domain beamforming gives a clearer map of transient signals. Source mapping is plotted by comparing the *Peak*and *RMS*output values, demonstrating that the *Peak*value achieves a better spatial resolution and MSL. The identification of impulsive sources is the main objective of [170], too. The classical delay-and-sum beamforming and numerical time-reversal techniques have been tested and compared for the localization of non–stationary, intermittent aeroacoustic sources.

5. Applications

5.1. Applications for moving sources identification: rotating machinery, pass-by and fly-over

An interesting application of beamforming is the one related to the identification of moving sources. Two works can be considered to be the milestones in this application field: the work of Howell [171] referring to aircraft fly-over and that of Barsikow [172] and Pallas for train pass-by. Both explore the main problem of the acoustics of moving sources: the emission frequency modification due to the Doppler effect. To take into account that effect, the de-Dopplerization of sound pressure is required. De-Dopplerization can be implemented by projecting the sound pressure acquired by the stationary array on a grid of point moving with the target object, as if their position changed in time at the same speed as the source. Pressure propagation is then performed sample by sample. For a good performance of this procedure, the relative position source-to-array must be known very accurately, synchronously with the acoustic data and for the whole duration of the experiment.

By considering a subsonic motion at Mach number M the pressure measured by the i^{th} microphone is:

$$p(x_i,t)=\frac{p(t-R_i(t)/c_0)}{4\pi R_i(t)(1-M\cos\theta(t))}, \tag{29}$$

where

$\theta(t)$ is the angle between the direction of observation and the source motion direction.

$R_i(t)$ is the distance between the i^{th} microphone and the source.

Source motion affects sound propagation and the actual pressure amplitude received by the microphone by a factor $(1 - M\cos\theta)$. If the sound is emitted by the source at a frequency f, the frequency received at the microphone position is f_D, the so-called Doppler frequency, and can be expressed as:

$$f_D = \frac{f}{(1 - M\cos\theta)}. \tag{30}$$

Beamforming on moving objects is usually performed in the time domain (see, for instance, [173]), but an implementation in the frequency domain was also proposed in [174] and in [175]. However, time domain processing has the advantage of being faster in the case of a large number of microphones. It practically consists of three steps:

1. the control point coordinates are calculated in the source coordinate system, so that they move fixed with the sound sources;
2. the sound pressures registered by the measurement microphones are processed in the source coordinate system and the Doppler frequency shift observed on the ground is removed (de-Dopplerization);
3. sound waves originating from the assumed source position are added up, following the conventional D&S procedure.

In this process, the microphone signals are interpolated for the time series given in the moving source reference system [171] and therefore the sampling rate of the data acquisition equipment should be at least four times higher than the maximum frequency of interest. Performance evaluation and uncertainty estimation of D&S for moving source emission evaluation was described in [176].

An approximate method based on the deconvolution of the beampattern of moving broadband sources was presented in [177] and in [178]. The method demonstrated a reasonable accuracy and computing time.

With regards to the field of rotating machinery, Sijtsma and Oerlemans ([179,180]) proposed a processing algorithm called ROSI (ROtating Source Identifier) and illustrated some applications to helicopter blades during hovering, aircraft and wind turbines. Dougherty et al. investigated fan blade noise [181] tested in an in-duct wind tunnel. They applied the CLEAN-SC algorithm to remove artifacts and improve array resolution. Wind turbine applications were also addressed by Gomes [182] and Bradley [183]. In the latter, high spatial resolution was achieved by exploiting a 40 m scale microphone array carrying 42 microphones. Sound pressure was sampled at 20 kHz to obtain high temporal resolution. In order to compensate the effects due to the large size of the test set–up (turbine, microphone array and their relative distance) and local wind variations, a reference speaker was mounted at the base of the turbine tower. It was used to determine the spatial characteristics of coherence and compensate for local wind variations.

Interesting applications to pass-by tests are discussed in [184], in relation to noise emission by passing-by cars, and in [185,186], where sound source localization on railway high speed trains is addressed. In [187] a method to perform pass–by tests using a 2-dimensional array is proposed and applied to the characterization of the noise emitted by a truck on road-side highway site.

Fly-over tests have been tackled by many authors, since they are very challenging due to the fact that acoustic sources move with very high speed, thus reducing the time to perform measurements. In [188] a hybrid time-frequency approach was described. The method presented is an evolution of DAMAS and takes into account Doppler frequency shift and modification of the point-spread functions due to source motion. The method is hybrid because beamforming is applied in the time domain while the PSFs used in DAMAS are calculated in the frequency domain, which drastically reduces the computational time and effort.

5.2. Wind tunnel applications

Wind tunnel array acoustics is probably the field in which beamforming has experienced major developments and has been validated in terms of functionality and accuracy of results [13]. Many algorithms developed for wind tunnel applications have been already described in Section 4 and therefore only peculiar cases will be presented hereafter. The first application of beamforming in wind tunnels is reported in [189]. A four- and eight-microphone linear array with "a digital time delay system" was developed to improve the directional response of the beamformer and reject background noise and reverberations produced by the closed section wind tunnel (the NASA Ames 40- by 80-ft wind tunnel). A noise rejection of 6 and 9 dB, respectively, was obtained, if compared with a conventional omnidirectional microphone with nose cone.

Aeroacoustic testing is typically carried out in open-jet or closed test-section wind tunnels. In open-jet wind tunnels the model is placed inside the potential core of the jet and the microphones are placed outside the flow. The sound waves radiated by the aeroacoustic sources located on the model surface have therefore to travel through the wind tunnel shear layer before being registered by the microphones. Those waves undergo sound speed gradients inducing refraction and scattering phenomena ([190,51]) and propagation based on the conventional Green function is no longer valid. This effect, quite similar to mirage in optics, was widely analyzed in [191], where an analytical formulation of the refraction by a planar and zero thickness shear layer was presented, based on geometrical acoustics. Amiet then introduced analytical expressions that make it possible to correct far-field measurement angle and acoustic amplitude for the effects of shear layer refraction. The correction is independent of the source type and the results represent the sound field one would expect to measure

in a flow that has a free stream extending to infinity. Despite some simplifications (e.g. the source is assumed to be in the centerline for the jet) this theory is still at the base of the correction algorithms used nowadays. More recently, the effects of shear layer were analyzed considering monopole sound sources placed at different position with respect to the jet centerline ([192]). The monopole sources were reproduced by acoustic signals generated by laser-induced plasmas. This study demonstrated that Amiet's method works properly when the source is in the jet-core or in a thin wake, while quantitative agreement degrades when the source is in a complex wake.

In closed test-section wind tunnels, which are widely used in aerodynamic tests, the main issue for aeroacoustic measurements is related to the fact that the hard walls of the test section produce reflections and degrade beamforming performances mainly in the low frequency range. Guidati et al. [193] presented an algorithm called *Reflection canceler*, which integrated a simple single-wall reflection model in the acoustic propagation formulation of the beamforming equation. Results demonstrated a good improvement in spatial resolution, with respect to standard algorithms based on free-field propagation, mainly at low frequencies. Before using the Reflection Canceller in real wind tunnel measurements, the steering vector calculated by the algorithm was validated with some basic experiments in [194]. The steering vector was measured using a simple test case, e.g. a monopole point source, in two simplified cases: in a closed test section wind tunnel without flow and in an acoustic conditioned wind tunnel with flow. The first test made it possible to confirm the effect of increased spatial resolution and the second one to compare the steering vectors measured with the modeled ones. Fenech et al. ([195]) proposed an image source method to improve beamforming accuracy in closed test-section wind tunnels by de-reverberating the measuring environment. Results demonstrated that this method is effective even when the wind tunnel geometry is not accurately modeled, provided that the number of image sources is chosen correctly.

An interesting application to cryogenic wind tunnel measurements was reported in [196]. Cryogenic wind-tunnels provide a significant increase in Reynolds number with no increase in dynamic pressure and tunnel power requirements: this allows a better similarity between the test results of a scaled model and those of the full-size object. An array has been developed for cryogenic application in the range of 100–300 K and the dependency of the sound power measured on Reynolds number was studied in-depth. The complete equipment was tested, demonstrating technical feasibility and long-term stability.

The aeroacoustic field has also been the theater of interesting developments trying to merge information coming from beamforming with other measurement data. An example of this is reported in [197], in which the sound pressure acquired by microphones array data were combined with the fluid–dynamic velocity measured by a contactless technique based on single–component Laser Doppler Anemometry (LDA) to calculate coherence beamforming (part of the map coherent with velocity data). The main issue was due to LDA irregular sampling intervals, dependent on the particle seeding which required specific data processing and data synchronization. The solution proposed was able to isolate the source related to local velocity. Another "data fusion" example was presented by Henning et al. in [198]. They combined beamforming with Particle Image Velocimetry (PIV) data (PIV is a measurement technique that measures the local velocity of a flow by observing the motion of particles seeding the fluid in a 2D or 3D space). This approach combined the advantages of both techniques: discriminating frequencies, which is typical of beamforming but difficult for PIV, discriminating phenomena in space with high resolution, which is typical of PIV but difficult for beamforming. By estimating the cross-correlation between the sound pressure calculated by BF, on the same spatial frame where the PIV measurement was performed, and the velocity, Henning et al. identified regular structures in the flow fluctuations and their relation to the sound field.

Apart from algorithms and data fusion strategies, the aeroacoustic field has also driven the innovation of array acoustics in terms of hardware solutions. Indeed, practical experience in beamforming has confirmed that, to make the design of a beamforming system more effective at the same cost, it is better to focus on the number of sensors rather than on their sensitivity and measurement accuracy. This assumption boosted the selection of hardware set-ups involving arrays with as low as possible channel costs, this including not only the sensors, but also the amplification and AD-converter chain. Micro-Electro-Mechanical-Systems (MEMS), mainly in their digital version with integrated signal digitization and coding, fully satisfy this need and have found many applications in recent times. In [199] the MEMS-based acoustic array technology was described. Humphreys et al. reported the latest advances in hardware and fabrication technologies, which have been exploited to realize an array of 128 MEMS microphones [200]. This array was used on an airplane model tested in a wind-tunnel, demonstrating a satisfactory overall performance. Further MEMS microphones array layouts, and their application to aeroacoustic source and urban noise pollution mapping were presented in [201] and in [202], respectively.

5.3. Application to Interior acoustics

Beamforming application to interior acoustics is definitely a challenge: conventional algorithms are typically founded on the hypothesis of a free-field propagation, however this hypothesis is, in most cases, no longer valid in an enclosed environment. Different strategies to tackle the issue caused by reflections inside closed environments have been proposed over the years. In [203], Chiariotti et al. applied the *Averaging beamforming* approach in a car cabin. They suggested to repeat the beamforming measurement by positioning the microphone array at different locations inside the cabin and then averaging out the beamforming maps obtained at each location of the array. The averaging process makes it possible to fade out the reflections of the cabin's hard walls appearing in the beamforming maps as "ghost sources", because their spatial location changes along that of the array. Guidati [204] proposed a processing method based on coherence filtering techniques aiming at distinguishing between the main source and incoherent sources and reflections or mirror sources. The coherence between

an additional sensor located close to the main source and the array microphones was used to filter the array signals, increasing the overall dynamic range of the acoustic map and filtering those parts of the radiated noise that were not coherent with the main source emission.

As discussed in 4.4, rigid spheres with flush mounted microphones are typically utilized to identify noise sources in 3-D environments like cabin interiors [205]. In [206] two inverse methods for interior sound source localization based on rigid spherical array measurements were presented. The first method was based on the iterative deconvolution of the beamforming pattern and equivalent source substitution; the second was based on the inversion of the acoustic transfer functions between the pressure measured by the microphones of the array and the volumetric velocities of the equivalent source distribution to be computed. The inversion was performed by applying the Tikhonov regularization method. By comparing the results of those two methods to conventional SHB, Schmitt and Lamotte demonstrated the improvement in spatial resolution of both the methods proposed. The inverse transfer function method showed very good performance in terms of resolution also in the low frequency range up to 400 Hz.

Acoustic beamforming was also applied by Nau et al. [207] for the understanding of the propagating sound field inside car cabins or on vehicle components. Since beamforming is limited in resolution in the low frequency range (i.e. below 500 Hz), it was supported and expanded with the use of sound intensity measurements.

A further application of interior acoustics is the in-duct application: Sijtsma [208] applied beamforming in a ducted parallel shear flow in which both flow speed and temperature vary in radial direction. The Green's functions of the acoustic differential equation in axisymmetric parallel shear flows have been used to construct steering vectors for in-duct beamforming with the aim to be used in the beamforming propagation equation. The same author proposed another solution for in-duct beamforming in [209], where he used Circular Harmonics Beamforming, i.e. where steering vectors decomposed into azimuthal modes were exploited rather than the Green's functions. An application to array beamforming inside turbofan engines was presented in that paper. An interesting application to mode identification in rectangular ducts by beamforming was presented a few years ago by Suzuki and Day [210]. They compared four different algorithms, conventional beamforming, CLEAN, L2 and L1 generalized-inverse beamforming to identify multiple acoustic duct modes. They proved that CLEAN, as well as L1/L2 inverse beamforming, outperform conventional beamforming, providing a 10 dB higher dynamic range in identifying duct modes.

Scientific literature also reports some works where this configuration was exploited in room acoustic applications. It is the case of the work of Park and Rafaely [211], who described an application to auditorium acoustics. They exploited an array of 98 microphones flush mounted over a rigid sphere to decompose the sound field into spherical harmonics up to the 6^{th} order and demonstrated the ability of SHB to identify and well separate direct sound and several reflections in an auditorium. Although the research activity to improve the accuracy of beamforming measurement in indoor environments is considerable, is worth citing the work of Dougherty et al. [212], who applied different beamforming methods (e.g. CB with diagonal suppression, individual processing of CSM eigenvectors, CLEAN-SC and reflections modeling by Green's function) to planar array measurements performed in a reverberation chamber, in order to assess the performances in terms of localization of acoustic sources. The authors concluded that conventional beamforming with a correction for the reverberant environment by means of the free-field Green's function provides satisfactory results. However, this is valid for a large environment like a standard reverberation room. It becomes more complicated if the environment is restricted like a vehicle cabin, primarily in cars.

5.4. Applications to machine diagnostics

An increasing interest has been demonstrated by the research community in trying to exploit acoustic beamforming to diagnose incipient/already developed faults machines. Antoni and his group can be considered pioneers in this sense. In [213] they combined time-domain beamforming and spectral kurtosis to detect faults in rotating machines. Since defects occurring in rotating machines have an impulsive nature, kurtosis, or impulsiveness factor, is a good index to detect their presence. Spectral kurtosis is a processing method for the identification of the frequency bands in which the impulsiveness of the signal is more important, which can be used to filter time domain data in order to keep the information only on the frequency range typical of the defect. Beamforming makes it possible to add spatial dimension, which combined with a spectral kurtosis filter makes it possible to localize impulsive sources in space. Angle domain beamforming is a methodology developed to localize sound sources produced by "cyclo-stationary" [214,215] systems. This means that the phenomena are random but they are repeating at each cycle at the same angular position, e.g. they are stationary cycle by cycle in a statistical sense. The acoustic image can be then averaged synchronously with the angular position thus allowing the removal of the random fluctuations of the microphones signals. One of the main applications of angle domain BF is to internal combustion engines, where it makes it possible to highlight mechanical borne noise with special focus on impulsive events, such as injection noise and piston slap. This approach is not based on angular sampling or on sampling at a fixed frequency in the time domain and then re-sampling in the angle domain. The instantaneous angular position or the rotation velocity is sampled together with the acoustic pressure and then the latter is averaged cycle after cycle, on the basis of the angular position. Every cycle will be angularly gated as a short signal for a given angular span, it representing a "sample" in the angular evolution along the entire cycle (e.g. in a four-strokes engine it takes 720 deg to be completed). The gated signal is then resampled in the time domain once again. Since gated time signals have a very short duration, a poor frequency resolution

is expected. This can be an issue for the beamforming analyses. Time domain data can be used to calculate the CSM and then beamforming maps by means of any kind of BF algorithm.

6. Concluding remarks

The aim of this paper was to present acoustic beamforming as approached by the authors over their years of investigation on this fascinating research topic. The document is not intended to represent neither a comprehensive nor a definitive review, for which the reader is redirected to dedicated monographs. However, a review collecting the most important papers and touching both basics and more advanced topics on acoustic beamforming could be useful for those approaching array acoustics for the first time as well for those already working in this field. For these reasons, beamforming has been presented starting from basic concepts and from the main criteria involved in the design of a beamforming test. The main beamforming strategies have been presented moving from "classical" approaches to more advanced and complex strategies. Some examples of the main applications of this measurement technique have also been provided, in order to give the reader an overview of the wide range of fields in which acoustic beamforming can be applied. Last but not least, the authors hope that the reading of this review might trigger the work of researchers in further evolving acoustic beamforming and exploiting it in applications which have not been tested yet.

Acknowledgments

The authors would like to thank Dr. Gianmarco Battista from Università Politecnica delle Marche and Dr. Claudio Colangeli from Siemens Industry Software for the precious help in collecting some references reported in this review paper.

References

[1] S. Gannot, E. Vincent, S. Markovich-Golan, A. Ozerov, A consolidated perspective on multimicrophone speech enhancement and source separation, IEEE/ACM Trans. Audio Speech Language Process. 25 (2017) 692–730, https://doi.org/10.1109/TASLP.2016.2647702.
[2] J. Billingsley, The acoustic telescope, J. Sound Vib. 48 (48) (1974) 485–510, https://doi.org/10.1016/0022-460X(76)90552-6.
[3] D. Doebler, G. Heilmann, Perspectives of the acoustic camera, in: International Congress on Noise Control Engineering 2005, INTERNOISE 2005, vol. 3, 2005, pp. 2672–2679.
[4] U. Michel, History of acoustic beamforming, in: 1st Berlin Beamforming Conference – 1st BeBeC, 2006.
[5] C.L. Dolph, A current distribution of broadside arrays which optimizes the relationship between beam width and sidelobe level, Inst. Radio Eng. 34 (1946) 335–348.
[6] R. Harrington, Sidelobe reduction by non-uniform element spacing, Inst. Radio Eng. Trans. Antennas Propag. 9 (1961) 187–201.
[7] T.T. Taylor, Design of line source antennas for narrow beam width and low sidelobes, IRE Trans. Antennas Propag. AP-3 (1955) 16–28.
[8] J. Capon, High-resolution frequency-wavenumber spectrum analysis, Proc. IEEE 57 (8) (1969) 1408–1418, https://doi.org/10.1109/proc.1969.7278.
[9] M.J. Fisher, M. Harper-Bourne, S.A.L. Glegg, Jet engine noise source location: the polar correlation technique, J. Sound Vib. 51 (1) (1977) 23–54, https://doi.org/10.1016/S0022-460X(77)80111-9.
[10] J. Billingsley, A comparison of the source location techniques of the acoustic telescope and polar correlation, J. Sound Vib. 61 (3) (1978) 419–425, https://doi.org/10.1016/0022-460X(78)90389-9.
[11] J.R. Williams, Fast beam-forming algorithm, J. Acoust. Soc. Am. 44 (44) (1968) 1454–1455, https://doi.org/10.1121/1.1911285.
[12] D.H. Johnson, D.E. Dudgeon, Array Signal Processing, Concepts and Techniques, P T R Prentice Hall, Englewood Cliffs, 1993.
[13] T.J. Mueller, Aeroacoustic Measurements, in: Experimental Fluid Mechanics, first ed., Springer-Verlag, Berlin Heidelberg, 2002.
[14] F. Marvasti, Nonuniform Sampling, Springer Us, 2001.
[15] B.D. Steinberg, Principles of Aperture and Array System Design, John Wiley & Sons, New York, 1976.
[16] R.A. Haubrich, Array design, Bull. Seismol. Soc. Am. 58 (3) (1968) 977–991.
[17] S. Holm, The coarray of sparse arrays with minimum sidelobe level, IEEE NORSIG-98 (1998) 137–140.
[18] G. Herold, E. Sarradj, An approach to estimate the reliability of microphone array methods, 21st AIAA/CEAS Aeroacoustics Conference, American Institute of Aeronautics and Astronautics, 2015, https://doi.org/10.2514/6.2015-2977.
[19] T. Brooks, W. Humphreys, Effect of directional array size on the measurement of airframe noise components, 5th AIAA/CEAS Aeroacoustics Conference and Exhibit, American Institute of Aeronautics and Astronautics, 1999, https://doi.org/10.2514/6.1999-1958.
[20] A. Nordborg, J. Wedemann, L. Willenbrink, Optimum array microphone configuration, International Congress and Exhibition on Noise Control Engineering, 4, Inter-Noise, 2000, pp. 2474–2478.
[21] J.-F. Piet, G. Elias, Airframe noise source localization using a microphone array, 3rd AIAA/CEAS Aeroacoustics Conference, American Institute of Aeronautics and Astronautics, 1997, https://doi.org/10.2514/6.1997-1643.
[22] J.J. Christensen, J. Hald, Beamforming – technical review no.1, Brüel & Kjaer, Technical Review 1–2004, 2004.
[23] C. Schulze, E. Sarradj, A. Zeibig, Characteristics of microphone arrays, in: International Congress and Exhibition on Noise Control Engineering, Inter-Noise, 2004.
[24] G. Elias, Source localization with a two-dimensional focussed array: optimal signal processing for a cross-shaped array, in: International Congress and Exhibition on Noise Control Engineering, Inter-Noise, 1995, pp. 1175–1178.
[25] R.P. Dougherty, Source location with sparse acoustic arrays: interference cancellation, Internal Report DNW (1997).
[26] R.P. Dougherty, Spiral-shaped array for broadband imaging, 1998.
[27] E.J.G. Arcondoulis, C.J. Doolan, A. Zander, L.A. Brooks, Design and calibration of a small aeroacoustic beamformer, 20th International Congress on Acoustics, ICA, 2010.
[28] J. Underbrink, Circularly symmetric, zero redundancy, planar array having broad frequency range applications, 2001.
[29] Z. Prime, C. Doolan, A comparison of popular beamforming arrays, Acoustics 2013 Victor Harbor: Science Technology and Amenity, Annual Conference of the Australian Acoustical Society, 2013, pp. 151–157.
[30] J. Christensen, J. Hald, Beamforming array of transducers, 2006.
[31] E. Sarradj, A generic approach to synthesize optimal array microphone arrangements, in: 6th Berlin Beamforming Conference – 6th BeBeC, 2016.
[32] A. Cigada, M. Lurati, F. Ripamonti, M. Vanali, Moving microphone arrays to reduce spatial aliasing in the beamforming technique: Theoretical background and numerical investigation, J. Acoust. Soc. Am. 124 (6) (2008) 3648–3658, https://doi.org/10.1121/1.2998778.
[33] A. Meyer, D. Doebler, Noise source localization within car interior using 3D-microphone arrays, in: 1st Berlin Beamforming Conference – 1st BeBeC, 2006.

[34] G. Heilmann, A. Meyer, D. Döbler, Time-domain beamforming using 3d-microphone arrays, in: 2nd Berlin Beamforming Conference – 2nd BeBeC, 2008.
[35] J.J. Bowman, T.B.A Senior, P.L.E. Uslenghi, Electromagnetic and acoustic scattering by simple shapes, North-Holland Pub. Co., 1970.
[36] F. Deblauwe, M. Robin, Capturing a noise source in an interior enclosure, NAG/DAGA (2009).
[37] E.G. Williams, Fourier Acoustics: Sound Radiation and Nearfield Acoustical Holography, Academic Press Inc., 1999, https://doi.org/10.1016/b978-0-12-753960-7.x5000-1.
[38] A. Lauterbach, K. Ehrenfried, L. Koop, S. Loose, Procedure for the accurate phase calibration of a microphone array, 15th AIAA/CEAS Aeroacoustics Conference (30th AIAA Aeroacoustics Conference), American Institute of Aeronautics and Astronautics, 2009, https://doi.org/10.2514/6.2009-3122.
[39] M. Mosher, M. Watts, S. Jovic, S. Jaeger, Calibration of microphone arrays for phased array processing, 3rd AIAA/CEAS Aeroacoustics Conference, American Institute of Aeronautics and Astronautics, 1997, https://doi.org/10.2514/6.1997-1678.
[40] D. Doebler, G. Heilmann, New method for positioning of microphones, in: 3rd Berlin Beamforming Conference – 3rd BeBeC, 2010.
[41] S. Kroeber, K. Ehrenfried, L. Koop, A. Lauterbach, In-flow calibration approach for improving beamforming accuracy, in: 3rd Berlin Beamforming Conference – 3rd BeBeC, 2010.
[42] M.J. Fisher, K.R. Holland, Measuring the relative strengths of a set of partially coherent acoustic sources, J. Sound Vib. 201 (1) (1997) 103–125, https://doi.org/10.1006/jsvi.1996.0743.
[43] E. Sarradj, Quantitative source spectra from acoustic array measurements, in: 2nd Berlin Beamforming Conference – 2nd BeBeC, 2008.
[44] E. Sarradj, A fast signal subspace approach for the determination of absolute levels from phased microphone array measurements, J. Sound Vib. 329 (9) (2010) 1553–1569, https://doi.org/10.1016/j.jsv.2009.11.009.
[45] H. Messer, Source localization performance and the array beampattern, Signal Process. 28 (2) (1992) 163–181, https://doi.org/10.1016/0165-1684(92)90033-S.
[46] P. Castellini, M. Martarelli, Acoustic beamforming: analysis of uncertainty and metrological performances, Mech. Syst. Signal Process. 22 (3) (2008) 672–692, https://doi.org/10.1016/j.ymssp.2007.09.017.
[47] T. Yardibi, C. Bahr, N. Zawodny, F. Liu, L.C.J. Li III, Uncertainty analysis of the standard delay-and-sum beamformer and array calibration, J. Sound Vib. 329 (13) (2010) 2654–2682, https://doi.org/10.1016/j.jsv.2010.01.014.
[48] L. Koop, K. Ehrenfried, S. Kroeber, Investigation of the systematic phase mismatch in microphone-array analysis, 11th AIAA/CEAS Aeroacoustics Conference, American Institute of Aeronautics and Astronautics, 2005, https://doi.org/10.2514/6.2005-2962.
[49] K. Ehrenfried, L. Koop, A. Henning, K. äpernick, Effects of wind-tunnel noise on array measurements in closed test section, in: 1st Berlin Beamforming Conference – 1st BeBeC, 2006.
[50] B. Fenech, K. Takeda, Beamforming accuracy in closed-section wind tunnels, 14th AIAA/CEAS Aeroacoustics Conference (29th AIAA Aeroacoustics Conference), American Institute of Aeronautics and Astronautics, 2008, https://doi.org/10.2514/6.2008-2908.
[51] P. Sijtsma, Acoustic array correction for coherence loss due to the wind tunnel shear layer, in: 2nd Berlin Beamforming Conference – 2nd BeBeC, 2008.
[52] P. Howells, Intermediate frequency side-lobe canceller, 1965.
[53] P. Applebaum, Adaptive arrays, IEEE Transactions on Antennas and Propagation 24 (SPL TR 66-1) (1966) 585–598, https://doi.org/10.1109/TAP.1976.1141417.
[54] B. Widrow, P. Mantey, L. Griffiths, B. Goode, Adaptive antenna systems, in: IEEE, vol. 55, Institute of Electrical and Electronics Engineers (IEEE), 1967, pp. 2143–2159.https://doi.org/10.1109/proc.1967.6092.
[55] I. Reed, J. Mallett, L. Brennan, Rapid convergence rate in adaptive arrays, IEEE Transactions on Aerospace and Electronic Systems AES-10 (vol. AES-10, no. 6), 1974, pp. 853–863.https://doi.org/10.1109/taes.1974.307893.
[56] O.L. Frost, An algorithm for linearly constrained adaptive array processing, IEEE 60 (8) (1972), 926–394.
[57] H.L. Van Trees, Detection, Estimation, and Modulation Theory, Part IV, Optimum Array Processing, John Wiley & Sons, New York, 2002.
[58] P. Stoica, Z. Wang, J. Li, Robust capon beamforming, IEEE Signal Process. Lett. 10 (6) (2003) 172–175, https://doi.org/10.1109/LSP.2003.811637.
[59] J. Li, P. Stoica, Z. Wang, On robust capon beamforming and diagonal loading, IEEE Trans. Signal Process. 51 (2003) 1702–1715, https://doi.org/10.1109/tsp.2003.812831.
[60] Y. Li, H. Ma, D. Yu, L. Cheng, Iterative robust capon beamforming, Signal Process. 118 (2016) 211–220, https://doi.org/10.1016/j.sigpro.2015.07.004.
[61] J.-L. Yu, C.-C. Yeh, Generalized eigenspace-based beamformers, IEEE Trans. Signal Process. 43 (11) (1995) 2453–2461, https://doi.org/10.1109/78.482097.
[62] J. Dmochowski, J. Benesty, S. Affes, Linearly constrained minimum variance source localization and spectral estimation, IEEE Trans. Audio Speech Language Process. 16 (8) (2008) 1490–1502, https://doi.org/10.1109/TASL.2008.2005029.
[63] G. Diodati, V. Quaranta, V. Fiorillo, F. Tarallo, F. Camastra, in: 24th International Congress on Sound and Vibration, ICSV, 2017.
[64] R.P. Dougherty, A new derivation of the adaptive beamforming formula, in: 7th Berlin Beamforming Conference – 7th BeBeC, 2018.
[65] E. Sarradj, C. Schulze, A. Zeibig, Identification of noise source mechanisms using orthogonal beamforming, in: Proceedings of Noise and Vibration Emerging Methods NOVEM, 2005, Saint Raphael, France.
[66] E. Sarradj, C. Schulze, Practical Application of Orthogonal Beamforming, in: 6th European Conference on Noise Control: Advanced Solutions for Noise Control, EURONOISE 2006, 2006.
[67] R.P. Dougherty, Functional beamforming, in: 5th Berlin Beamforming Conference – 5th BeBeC, 2014.
[68] R. Merino-Martinez, M. Snellen, D.G. Simons, Functional beamforming applied to full scale landing aircraft, in: 6th Berlin Beamforming Conference – 6th BeBeC, 2016.
[69] Y. Yang, Z. Chu, L. Shen, Z. Xu, Functional delay and sum beamforming for three-dimensional acoustic source identification with solid spherical arrays, J. Sound Vib. 373 (2016) 340–359, https://doi.org/10.1016/j.jsv.2016.03.024.
[70] S. Guidati, R. Sottek, Advanced source localization techniques using microphone arrays, SAE Int. J. Passenger Cars – Mech. Syst. 4 (2) (2011) 1241–1249, https://doi.org/10.4271/2011-01-1657.
[71] B. Beguet, L. Lamotte, Device for localizing acoustic sources and measuring their intensities, 2007.
[72] L. Lamotte, B. Beguet, C. Cariou, O. Delverdier, Qualifying the noise sources in term of localization and quantification during flight tests, European Conference for AeroSpace Sciences – EUCASS2009 (2009).
[73] R.J. Urick, Principles of Underwater Sound, third ed., Mc Graw-Hill Book Company, 1983.
[74] R. Porteous, Z. Prime, C.J. Doolan, D.J. Moreau, V. Valeau, Three-dimensional beamforming of dipolar aeroacoustic sources, J. Sound Vib. 355 (2015) 117–134, https://doi.org/10.1016/j.jsv.2015.06.030.
[75] C. Cariou, O. Delverdier, S. Paillasseur, L. Lamotte, Tool for interior noise sources detection in aircraft with comparison of configuration, 4th Berlin Beamforming Conference – 4th BeBeC (2012).
[76] L. Lamotte, O. Minck, S. Paillasseur, J. Lanslot, F. Deblauwe, Interior noise source identification with multiple spherical arrays in aircraft and vehicle, in: 20th International Congress on Sound and Vibration 2013, ICSV 2013, vol. 1, 2013, pp. 451–458.
[77] P. Castellini, A. Sassaroli, Acoustic source localization in a reverberant environment by average beamforming, Mech. Syst. Signal Process. 24 (3) (2010) 796–808, https://doi.org/10.1016/j.ymssp.2009.10.021.
[78] J.A. Hogbom, Aperture synthesis with a non-regular distribution of interferometer baselines, Astron. Astrophys. Suppl. 15 (1974) 417–426.
[79] G.M. Skofronick-Jackson, A.J. Gasiewski, in: Proceedings of the 1995 International Geosciences and Remote Sensing Symposium, 1995, pp. 1898–1900.
[80] R.P. Dougherty, R. Stoker, Sidelobe suppression for phased array aeroacoustic measurements, in: 4th AIAA/CEAS Aeroacoustics Conference, American Institute of Aeronautics and Astronautics, 1998, https://doi.org/10.2514/6.1998-2242.
[81] P. Sijtsma, Clean based on spatial source coherence, Int. J. Aeroacoustics 6 (4) (2007) 357–374, https://doi.org/10.1260/147547207783359459.
[82] P. Sijtsma, Clean based on spatial source coherence – NLR-TP-2007-345 Tech. rep, National Aerospace Laboratory NLR, 2007.

[83] A. Quayle, W. Graham, A. Dowling, H. Babinsky, Y. Liu, Mitigation of beamforming interference from closed wind tunnels using CLEAN-SC, in: 2nd Berlin Beamforming Conference – 2nd BeBeC, 2008.
[84] P. Sijtsma, M. Snellen, High-resolution CLEAN-SC, in: 6th Berlin Beamforming Conference – 6th BeBeC, 2016.
[85] T.F. Brooks, W.M. Humphreys, A deconvolution approach for the mapping of acoustic sources (DAMAS) determined from phased microphone arrays, in: 10th AIAA/CEAS Aeroacoustics Conference, American Institute of Aeronautics and Astronautics, 2004, https://doi.org/10.2514/6.2004-2954.
[86] T.F. Brooks, W.M. Humphreys, Extension of damas phased array processing for spatial coherence determination (damas-c), 12th AIAA/CEAS Aeroacoustics Conference.https://doi.org/10.2514/6.2006-2654.
[87] R.P. Dougherty, Extensions of DAMAS and benefits and limitations of deconvolution in beamforming, in: 11th AIAA/CEAS Aeroacoustics Conference, American Institute of Aeronautics and Astronautics, 2005, https://doi.org/10.2514/6.2005-2961.
[88] L. Brusniak, DAMAS2 validation for flight test airframe noise measurements, in: 2nd Berlin Beamforming Conference – 2nd BeBeC, 2008.
[89] T. Suzuki, DAMAS2 using a point-spread function weakly varying in space, AIAA J. 48 (9) (2010) 2165–2169, https://doi.org/10.2514/1.51674.
[90] O. Jiříček, Aeroacoustics research in europe: the CEAS-ASC report on 2015 highlights, J. Sound Vib. 381 (2016) 101–120, https://doi.org/10.1016/j.jsv.2016.06.029.
[91] T. Spalt, C. Fuller, T. Brooks, W. Humphreys, A background noise reduction technique using adaptive noise cancellation for microphone arrays, in: 17th AIAA/CEAS Aeroacoustics Conference (32nd AIAA Aeroacoustics Conference), American Institute of Aeronautics and Astronautics, 2011, https://doi.org/10.2514/6.2011-2715.
[92] C.L. Lawson, R.J. Hanson, Solving least squares problems (classics in applied mathematics), Soc. Ind. Appl. Math. (1987), https://doi.org/10.1137/1.9781611971217.
[93] W.H. Richardson, Bayesian-based iterative method of image restoration, J. Opt. Soc. Am. 62 (1972) 55–59, https://doi.org/10.1364/JOSA.62.000055.
[94] L.B. Lucy, An iterative technique for the rectification of observed distributions, Astron. J. 79 (1974) 745, https://doi.org/10.1086/111605.
[95] D.A. Fish, J.G. Walker, A.M. Brinicombe, E.R. Pike, Blind deconvolution by means of the richardson-lucy algorithm, J. Opt. Soc. Am. A 12 (1) (1995) 58, https://doi.org/10.1364/josaa.12.000058.
[96] K. Ehrenfried, L. Koop, A comparison of iterative deconvolution algorithms for the mapping of acoustic sources, in: 12th AIAA/CEAS Aeroacoustics Conference (27th AIAA Aeroacoustics Conference), American Institute of Aeronautics and Astronautics, 2006, https://doi.org/10.2514/6.2006-2711.
[97] Z. Chu, Y. Yang, Comparison of deconvolution methods for the visualization of acoustic sources based on cross-spectral imaging function beamforming, Mech. Syst. Signal Process. 48 (12) (2014) 404–422, https://doi.org/10.1016/j.ymssp.2014.03.012.
[98] P.A. Ravetta, R.A. Burdisso, W.F. Ng, Noise source localization and optimization of phased-array results, in: 12th AIAA/CEAS Aeroacoustics Conference, vol. 47, American Institute of Aeronautics and Astronautics (AIAA), 2009, pp. 2520–2533.https://doi.org/10.2514/1.38073.
[99] C. Bahr, L. Cattafesta, Wavespace-based coherent deconvolution, in: 18th AIAA/CEAS Aeroacoustics Conference (33rd AIAA Aeroacoustics Conference), in: 18th AIAA/CEAS Aeroacoustics Conference (33rd AIAA Aeroacoustics Conference), Aeroacoustics Conference, American Institute of Aeronautics and Astronautics, 2012, https://doi.org/10.2514/6.2012-2227.
[100] J.D. Maynard, E.G. Williams, Y. Lee, Nearfield acoustic holography: I. theory of generalized holography and the development of nah, J. Acoust. Soc. Am. 78 (1985) 1395–1413, https://doi.org/10.1121/1.392911.
[101] J. Hald, Patch near-field acoustical holography using a new statistically optimal method, in: International Congress and Exhibition on Noise Control Engineering, Inter-Noise, 2003.
[102] J. Hald, Basic theory and properties of statistically optimized near-field acoustical holography, J. Acoust. Soc. Am. 125 (4) (2009) 2105–2120, https://doi.org/10.1121/1.3079773.
[103] Z. Wang, S.F. Wu, Helmholtz equation-least-squares method for reconstructing the acoustic pressure field, J. Acoust. Soc. Am. 102 (4) (1997) 2020–2032, https://doi.org/10.1121/1.419691.
[104] S.F. Wu, On reconstruction of acoustic pressure fields using the helmholtz equation least squares method, J. Acoust. Soc. Am. 107 (5) (2000) 2511–2522, https://doi.org/10.1121/1.428639.
[105] M.R. Bai, Application of BEM (boundary element method)-based acoustic holography to radiation analysis of sound sources with arbitrarily shaped geometries, J. Acoust. Soc. Am. 92 (1) (1992) 533–549, https://doi.org/10.1121/1.404263.
[106] B.-K. Kim, J.-G. Ih, On the reconstruction of the vibro-acoustic field over the surface enclosing an interior space using the boundary element method, J. Acoust. Soc. Am. 100 (5) (1996) 3003–3016, https://doi.org/10.1121/1.417112.
[107] A. Sarkissian, Method of superposition applied to patch near-field acoustic holography, J. Acoust. Soc. Am. 118 (2) (2005) 671–678, https://doi.org/10.1121/1.1945470.
[108] G.H. Koopmann, L. Song, J.B. Fahnline, A method for computing acoustic fields based on the principle of wave superposition, J. Acoust. Soc. Am. 86 (6) (1989) 2433–2438, https://doi.org/10.1121/1.398450.
[109] S. Lee, Review: the use of equivalent source method in computational acoustics, J. Comput. Acoust. 25 (1).https://doi.org/10.1142/s0218396x16300012.
[110] Q. Leclère, A. Pereira, C. Bailly, J. Antoni, C. Picard, A unified formalism for acoustic imaging techniques: illustrations in the frame of a didactic numerical benchmark, in: 6th Berlin Beamforming Conference - 6th BeBeC, 2016.
[111] T. Yardibi, J. Li, P. Stoica, L.N. Cattafesta, Sparsity constrained deconvolution approaches for acoustic source mapping, J. Acoust. Soc. Am. 123 (5) (2008) 2631–2642, https://doi.org/10.1121/1.2896754.
[112] G. Herold, E. Sarradj, T. Geyer, Covariance matrix fitting for aeroacoustic application, in: Fortschritte der Akustik – AIA-DAGA 2013, 2013, pp. 1926–1928.
[113] P.C. Hansen, Regularization tools: A matlab package for analysis and solution of discrete ill-posed problems, Numerical Algorithms 6 (1) (1994) 1–35, https://doi.org/10.1007/BF02149761.
[114] J. Hadamard, Sur les problèmes aux dérivés partielles et leur signification physique, Princeton University Bulletin 13 (1902) 49–52.
[115] A.N. Tikhonov, Solution of incorrectly formulated problems and the regularization method, Soviet Math. Dokl. 4 (1963) 1035–1038.
[116] T. Padois, P.-A. Gauthier, A. Berry, Inverse problem with beamforming regularization matrix applied to sound source localization in closed wind-tunnel using microphone array, J. Sound Vib. 333 (25) (2014) 6858–6868.
[117] A. Pereira, Acoustic imaging in enclosed spaces, INSA de Lyon (2014) (Ph.D. thesis).
[118] A. Pereira, Q. Leclère, Improving the Equivalent Source Method for noise source identification in enclosed spaces, in: 18th International Congress on Sound and Vibration (ICSV 18), Brazil, 2011, p. R31.
[119] Y.C. Pati, R. Rezaiifar, P.S. Krishnaprasad, Orthogonal matching pursuit: Recursive function approximation with applications to wavelet decomposition, in: in Conference Record of The Twenty-Seventh Asilomar Conference on Signals, Systems and Computers, 1993, pp. 1–3.
[120] R. Rubinstein, M. Zibulevsky, M. Elad, Efficient implementation of the K-SVD algorithm using batch orthogonal matching pursuit, Tech. Rep. (2008).
[121] P. Boufounos, M.F. Duarte, R.G. Baraniuk, Sparse signal reconstruction from noisy compressive measurements using cross validation, in: 2007 IEEE/SP 14th Workshop on Statistical Signal Processing, IEEE, 2007, https://doi.org/10.1109/ssp.2007.4301267.
[122] R. Tibshirani, I. Johnstone, T. Hastie, B. Efron, Least angle regression, Ann. Stat. 32 (2) (2004) 407–499, https://doi.org/10.1214/009053604000000067.
[123] T. Suzuki, Generalized inverse beamforming algorithm resolving coherent/incoherent, distributed and multipole sources, J. Sound Vib. 330 (24) (2011) 5835–5851, https://doi.org/10.1016/j.jsv.2011.05.021.
[124] P.A.G. Zavala, W.D. Roeck, K. Janssens, J. Arruda, P. Sas, W. Desmet, Generalized inverse beamforming investigation and hybrid estimation, in: 3rd Berlin Beamforming Conference - 3rd BeBeC, 2010.
[125] P.A.G. Zavala, W.D. Roeck, K. Janssens, J.R.F. Arruda, P. Sas, W. Desmet, Generalized inverse beamforming with optimized regularization strategy, Mech. Syst. Signal Process. 25 (3) (2011) 928–939.

[126] F. Presezniak, P.A.G. Zavala, G. Steenackers, K. Janssens, J.R.F. Arruda, W. Desmet, P. Guillaume, Acoustic source identification using a generalized weighted inverse beamforming technique, Mech. Syst. Signal Process. 32 (2012) 349–358, https://doi.org/10.1016/j.ymssp.2012.06.019.
[127] C. Colangeli, P. Chiariotti, K. Janssens, Uncorrelated noise sources separation using inverse beamforming, Experimental Techniques, Rotating Machinery, and Acoustics, vol. 8, Springer, 2015, pp. 59–70.
[128] R.P. Dougherty, Improved generalized inverse beamforming for jet noise, Int. J. Aeroacoustics 11 (3–4) (2012) 259–290, https://doi.org/10.1260/1475-472X.11.3-4.259.
[129] R. Chartrand, W. Yin, Iteratively reweighted algorithms for compressive sensing, in: 2008 IEEE International Conference on Acoustics, Speech and Signal Processing, IEEE, 2008, https://doi.org/10.1109/icassp.2008.4518498.
[130] I. Daubechies, R. DeVore, M. Fornasier, S. Güntürk, Iteratively reweighted least squares minimization for sparse recovery, Commun. Pure Appl. Math. 63 (1) (2010) 1–38, https://doi.org/10.1002/cpa.20303.
[131] J. Antoni, A bayesian approach to sound source reconstruction: optimal basis, regularization, and focusing, J. Acoust. Soc. Am. 131 (4) (2012) 2873–2890, https://doi.org/10.1121/1.3685484.
[132] A. Pereira, Q. Leclère, J. Antoni, A theoretical and experimental comparison of the equivalent source method and a bayesian approach to noise source identification, in: 4th Berlin Beamforming Conference – 4th BeBeC, 2012.
[133] A. Pereira, J. Antoni, Q. Leclère, Empirical bayesian regularization of the inverse acoustic problem, Appl. Acoust. 97 (2015) 11–29, https://doi.org/10.1016/j.apacoust.2015.03.008.
[134] P. Castellini, F. Sopranzetti, Phase mapping of acoustic sources by beamforming and iterative far field monopole substitution, J. Acoust. Soc. Am. 132 (1) (2012) 295–302.
[135] B. Rafaely, Fundamentals of Spherical Array Processing, Springer Berlin Heidelberg, 2015, https://doi.org/10.1007/978-3-662-45664-4.
[136] I.H. Sloan, R.S. Womersley, Extremal systems of points and numerical integration on the sphere, Adv. Comput. Math. 21 (1/2) (2004) 107–125, https://doi.org/10.1023/B:ACOM.0000016428.25905.da.
[137] J. Meyer, Beamforming for a circular microphone array mounted on spherically shaped objects, J. Acoust. Soc. Am. 109 (1) (2001) 185–193, https://doi.org/10.1121/1.1329616.
[138] J. Meyer, G. Elko, A highly scalable spherical microphone array based on an orthonormal decomposition of the soundfield, in: IEEE International Conference on Acoustics Speech and Signal Processing, IEEE, 2002, https://doi.org/10.1109/icassp.2002.5744968.
[139] J. Meyer, G.W. Elko, Eigenbeam beamforming for microphone arrays, J. Acoust. Soc. Am. 120 (5) (2006), https://doi.org/10.1121/1.4787960, 3177–3177.
[140] B. Rafaely, Plane-wave decomposition of the sound field on a sphere by spherical convolution, J. Acoust. Soc. Am. 116 (4I) (2004) 2149–2157, https://doi.org/10.1121/1.1792643.
[141] B. Rafaely, Analysis and design of spherical microphone arrays, IEEE Trans. Speech Audio Process. 13 (1) (2005) 135–143, https://doi.org/10.1109/TSA.2004.839244.
[142] B. Rafaely, Phase-mode versus delay-and-sum spherical microphone array processing, IEEE Signal Process. Lett. 12 (10) (2005) 713–716, https://doi.org/10.1109/LSP.2005.855542.
[143] B. Rafaely, B. Weiss, E. Bachmat, Spatial aliasing in spherical microphone arrays, IEEE Trans. Signal Process. 55 (3) (2007) 1003–1010, https://doi.org/10.1109/TSP.2006.888896.
[144] Z. Li, R. Duraiswami, Flexible and optimal design of spherical microphone arrays for beamforming, IEEE Trans. Audio Speech Lang. Process. 15 (2) (2007) 702–714, https://doi.org/10.1109/TASL.2006.876764.
[145] M. Brandstein, D. Ward, Microphone Arrays, Springer Berlin Heidelberg, 2001, https://doi.org/10.1007/978-3-662-04619-7.
[146] K. Haddad, J. Hald, 3d localization of acoustic sources with a spherical array, J. Acoust. Soc. Am. 123 (5) (2008), https://doi.org/10.1121/1.2933754, 3311–3311.
[147] J. Hald, Spherical beamforming with enhanced dynamic range, SAE Technical Paper, 2013, Tech. rep.
[148] E. Tiana-Roig, A. Torras-Rosell, E. Fernandes-Grande, C. Jeong, F. Agerkvist, Enhancing the beamforming map of spherical arrays at low frequencies using acoustic holography, in: 5th Berlin Beamforming Conference – 5th BeBeC, 2014.
[149] Z. Chu, Y. Yang, Y. He, Deconvolution for three-dimensional acoustic source identification based on spherical harmonics beamforming, J. Sound Vib. 344 (2015) 484–502, https://doi.org/10.1016/j.jsv.2015.01.047.
[150] G. Battista, P. Chiariotti, P. Castellini, Spherical harmonics decomposition in inverse acoustic methods involving spherical arrays, J. Sound Vib. 433 (2018) 425–460, https://doi.org/10.1016/j.jsv.2018.05.001.
[151] M. Maffei, A. Bianco, Improvements of the beamforming technique in pininfarina full scale wind tunnel by using a 3D scanning system, SAE Int. J. Mater. Manf. 1 (2008) 154–168, https://doi.org/10.4271/2008-01-0405.
[152] D. Doebler, J. Ocker, C. Puhle, On 3d beamforming in the wind tunnel, in: 6th Berlin Beamforming Conference – 6th BeBeC, 2016.
[153] T. Brooks, W. Humphreys, Three-dimensional applications of DAMAS methodology for aeroacoustic noise source definition, in: 11th AIAA/CEAS Aeroacoustics Conference, American Institute of Aeronautics and Astronautics, 2005, https://doi.org/10.2514/6.2005-2960.
[154] R.P. Dougherty, in: in: 3rd Berlin Beamforming Conference – 3rd BeBeC, 2010.
[155] M. Legg, S. Bradley, Comparison of CLEAN-SC for 2D and 3D scanning surfaces, in: 4th Berlin Beamforming Conference – 4th BeBeC, 2012.
[156] T. Geyer, E. Sarradj, J. Giesler, Application of a beamforming technique to the measurement of airfoil leading edge noise, Adv. Acoust. Vib. 2012 (905461) (2012) 1–16, https://doi.org/10.1155/2012/905461.
[157] E. Sarradj, Three-dimensional acoustic source mapping, in: 4th Berlin Beamforming Conference – 4th BeBeC, 2012.
[158] E. Sarradj, Three-dimensional acoustic source mapping with different beamforming steering vector formulations, Adv. Acoust. Vib. 2012 (292695) (2012) 1–12, https://doi.org/10.1155/2012/292695.
[159] A. Xenaki, F. Jacobsen, E. Fernandez-Grande, Improving the resolution of three-dimensional acoustic imaging with planar phased arrays, J. Sound Vib. 331 (8) (2012) 1939–1950, https://doi.org/10.1016/j.jsv.2011.12.011.
[160] T. Padois, A. Berry, Two and three-dimensional sound source localization with beamforming and several deconvolution techniques, Acta Acustica united with Acustica 103 (3) (2017) 392–400, https://doi.org/10.3813/AAA.919069.
[161] F. Ning, J. Wei, L. Qiu, H. Shi, X. Li, Three-dimensional acoustic imaging with planar microphone arrays and compressive sensing, J. Sound Vib. 380 (2016) 112–128, https://doi.org/10.1016/j.jsv.2016.06.009.
[162] G. Battista, P. Chiariotti, G. Herold, E. Sarradj, P. Castellini, Inverse methods for three-dimensional acoustic mapping with a single planar array, in: 7th Berlin Beamforming Conference – 7th BeBeC, 2018.
[163] J. Stier, C. Hahn, G. Zechel, M. Beitelschmidt, Computational optimization of a time-domain beamforming algorithm using cpu and gpu, in: 5th Berlin Beamforming Conference – 5th BeBeC, 2014.
[164] O. Jaeckel, Strengths and weaknesses of calculating beamforming in the time domain, in: 1st Berlin Beamforming Conference – 1st BeBeC, 2006.
[165] R.P. Dougherty, Advanced time-domain beamforming techniques, in: 10th AIAA/CEAS Aeroacoustics Conference, American Institute of Aeronautics and Astronautics, 2004, https://doi.org/10.2514/6.2004-2955.
[166] D. Doebler, R. Schroeder, Contrast improvement and source separation enhancement using high dynamic range algorithm, in: 4th Berlin Beamforming Conference – 4th BeBeC, 2012.
[167] N. Quaegebeur, T. Padois, P.-A. Gauthier, P. Masson, Enhancement of time-domain acoustic imaging based on generalized cross-correlation and spatial weighting, Mech. Syst. Signal Process. 75 (2016) 515–524, https://doi.org/10.1016/j.ymssp.2015.12.012.
[168] D.-H. Seo, J.-W. Choi, Y.-H. Kim, Impulsive sound source localization using peak and {RMS} estimation of the time-domain beamformer output, Mech. Syst. Signal Process. 49 (12) (2014) 95–105, https://doi.org/10.1016/j.ymssp.2014.03.013.

[169] Y.-C. Choi, Y.-H. Kim, Impulsive sources localisation in noisy environment using modified beamforming method, Mech. Syst. Signal Process. 20 (6) (2006) 1473–1481, https://doi.org/10.1016/j.ymssp.2005.04.011.
[170] J. Fischer, I. Rakotoarisoa, V. Valeau, D. Marx, C. Prax, L. Brizzi, Time-domain imaging techniques for aerocoustic sources, in: 6th Berlin Beamforming Conference – 6th BeBeC, 2016.
[171] G.P. Howell, M.A. Bradley, M.A. McCormick, J.D. Brown, De-Dopplerization and acoustic imaging of aircraft Flyover noise measurements, J. Sound Vib. 105 (1) (1986) 151–167, https://doi.org/10.1016/0022-460X(86)90227-0.
[172] B. Barsikow, W.F. King III, On removing the doppler frequency shift from array measurements of railway noise, J. Sound Vib. 120 (1) (1988) 190–196, https://doi.org/10.1016/0022-460X(88)90344-6, letter to the editor.
[173] P. Sijtsma, Experimental techniques for identification and characterization of noise sources, Adv. Aeroacoustics Appl. VKI Lecture Series (2004) 1–47.
[174] H.E. Camargo, A frequency domain beamforming method to locate moving sound sources Ph.D. thesis, Virginia Polytechnic Institute and State University, Blacksburg, 2010.
[175] S. Guerin, C. Weckmueller, Frequency-domain reconstruction of the point-spread function for moving sources, in: 2nd Berlin Beamforming Conference – 2nd BeBeC, 2008.
[176] A. Cigada, F. Ripamonti, M. Vanali, The delay & sum algorithm applied to microphone array measurement: Numerical analysis and experimental validation, Mech. Syst. Signal Process. 21 (6) (2007) 2645–2664, https://doi.org/10.1016/j.ymssp.2007.01.001.
[177] S. Guerin, C. Weckmueller, U. Michel, Beamforming and deconvolution for aerodynamic sound sources in motion, in: 1st Berlin Beamforming Conference – 1st BeBeC, 2006.
[178] L. Lamotte, B. Nicolas, M. Pham, B. Oudompheng, A theoretical and experimental comparison of the deconvolution methods for moving sources, in: 6th Berlin Beamforming Conference – 6th BeBeC, 2016.
[179] P. Sijtsma, S. Oerlemans, H. Holthusen, Location of rotating sources by phased array measurements, in: 7th AIAA/CEAS Aeroacoustics Conference and Exhibit, American Institute of Aeronautics and Astronautics, 2001, https://doi.org/10.2514/6.2001-2167.
[180] S. Oerlemans, Detection of Aeroacoustic Sound Sources on Aircraft and Wind Turbines Phd thesis, University of Twente, Enschede, 2009.
[181] R.P. Dougherty, B. Walker, Virtual rotating microphone imaging of broadband fan noise, in: 15th AIAA/CEAS Aeroacoustics Conference (30th AIAA Aeroacoustics Conference), American Institute of Aeronautics and Astronautics, 2009, https://doi.org/10.2514/6.2009-3121.
[182] J. Gomes, Noise source identification with blade tracking on a wind turbine, in: 41st International Congress and Exhibition on Noise Control Engineering, Inter-Noise 2012, 2012, internoise 2012, August 19-22, New York City, NY, USA.
[183] S. Bradley, T. Mikkelsen, S. von Huenerbein, M. Legg, Precision measurements of windd turbine noise using a large aperture microphone array, in: 6th Berlin Beamforming Conference – 6th BeBeC, 2016.
[184] Y. Takano, K. Terada, E. Aizawa, A. Iida, H. Fujita, Development of a 2-dimensional microphone array measurement system for noise sources of fast moving vehicles, International Congress and Exhibition on Noise Control Engineering, Inter-Noise (1992) 1175–1178.
[185] S. Brühl, K.-P. Schmitz, Noise Source Localization on Highspeed Trains Using Different Array Types, in: International Congress and Exhibition on Noise Control Engineering, Inter-Noise, 1993, pp. 1311–1314.
[186] B. Barsikow, Experiences with various configurations of microphone arrays used to locate sound sources on railway trains operated by the DB AG, J. Sound Vib. 193 (1996) 283–293, https://doi.org/10.1006/jsvi.1996.0269.
[187] W. Blake, P. Donovan, A new road-side array-. Based method for characterization of truck noise during passby, Am. Soc. Mech. Eng. (2008).
[188] S. Guerin, H. Siller, A hybrid time-frequency approach for the noise localization analysis of aircraft fly-overs, in: 14th AIAA/CEAS Aeroacoustics Conference (29th AIAA Aeroacoustics Conference), American Institute of Aeronautics and Astronautics, 2008, https://doi.org/10.2514/6.2008-2955.
[189] P.S.S. Noble, A directional microphone array for acoustic studies of wind tunnel models, in: 8th Aerodynamic Testing Conference, American Institute of Aeronautics and Astronautics, 1974, https://doi.org/10.2514/6.1974-640.
[190] R.H. Schlinker, R.K. Amiet, Refraction and scattering of sound by a shear layer, in: 6th Aeroacoustics Conference, American Institute of Aeronautics and Astronautics, 1980, https://doi.org/10.2514/6.1980-973.
[191] R.K. Amiet, Correction of open-jet wind-tunnel measurements for shear layer refraction, in: 2nd Aeroacoustics Conference, American Institute of Aeronautics and Astronautics, 1976, pp. 259–280, https://doi.org/10.2514/5.9781600865206.0259.0280.
[192] C. Bahr, N.S. Zawodny, T. Yardibi, F. Liu, D. Wetzel, B. Bertolucci, L. Cattafesta, Shear layer time-delay correction using a non-intrusive acoustic point source, Int. J. Aeroacoustics 10 (5–6) (2011) 497–530, https://doi.org/10.1260/1475-472x.10.5-6.497.
[193] S. Guidati, C. Brauer, S. Wagner, The reflection canceller – phased array measurements in a reverberating environment, in: 8th AIAA/CEAS Aeroacoustics Conference & Exhibit, American Institute of Aeronautics and Astronautics, 2002, https://doi.org/10.2514/6.2002-2462.
[194] S. Guidati, G. Guidati, S. Wagner, Beamforming in a reverberating environment with the use of measured steering vectors, in: 7th AIAA/CEAS Aeroacoustics Conference and Exhibit, American Institute of Aeronautics and Astronautics, 2001, https://doi.org/10.2514/6.2001-2166.
[195] B. Fenech, K. Takeda, Towards more accurate beamforming levels in closed-section wind tunnels via de-reverberation, in: 13th AIAA/CEAS Aeroacoustics Conference (28th AIAA Aeroacoustics Conference), American Institute of Aeronautics and Astronautics, 2007, https://doi.org/10.2514/6.2007-3431.
[196] T. Ahlefeldt, L. Koop, Microphone-array measurements in a cryogenic wind tunnel, AIAA J. 48 (7) (2010) 1470–1479, https://doi.org/10.2514/1.50871.
[197] M. Garcia-Pedroche, G. Bennett, Aeroacoustic noise source identification using irregularly sampled LDV measurements coupled with beamforming, in: 17th AIAA/CEAS Aeroacoustics Conference (32nd AIAA Aeroacoustics Conference), American Institute of Aeronautics and Astronautics, 2011, https://doi.org/10.2514/6.2011-2719.
[198] A. Henning, L. Koop, K. Ehrenfried, A. Lauterbach, S. Kröber, Simultaneous multiplane PIV and microphone array measurements on a rod-airfoil configuration, in: 15th AIAA/CEAS Aeroacoustics Conference (30th AIAA Aeroacoustics Conference), American Institute of Aeronautics and Astronautics, 2009, https://doi.org/10.2514/6.2009-3184.
[199] T. Nishida, L. Cattafest, M. Sheplak, D. Arnold, MEMS-based acoustic array technology, in: 40th AIAA Aerospace Sciences Meeting & Exhibit, American Institute of Aeronautics and Astronautics, 2002, https://doi.org/10.2514/6.2002-253.
[200] W. Humphreys, Q. Shams, S. Graves, B. Sealey, S. Bartram, T. Comeaux, Application of MEMS microphone array technology to airframe noise measurements, in: 11th AIAA/CEAS Aeroacoustics Conference, American Institute of Aeronautics and Astronautics, 2005, https://doi.org/10.2514/6.2005-3004.
[201] S. Orlando, A. Bale, D. Johnson, Design and preliminary testing of a MEMS microphone phased array, in: 3rd Berlin Beamforming Conference – 3rd BeBeC, 2010.
[202] J. Tiete, F. Domínguez, B. da Silva, L. Segers, K. Steenhaut, A. Touhafi, Soundcompass: a distributed mems microphone array-based sensor for sound source localization, Sensors 14 (2) (2014) 1918–1949, https://doi.org/10.3390/s140201918.
[203] P. Chiariotti, G. Battista, M. Ettorre, P. Castellini, Average acoustic beamforming in car cabins: an automatic system for acoustic mapping over 3d surfaces, Appl. Acoust. 129 (2018) 47–63, https://doi.org/10.1016/j.apacoust.2017.07.009.
[204] S. Guidati, Advanced beamfoming techniques in vehicle acoustics, in: 3rd Berlin Beamforming Conference – 3rd BeBeC, 2010.
[205] Y.-C. Choi, J.-H. Park, D.-B. Yoon, H.-S. Kwon, Noise source identification in a reverberant field using spherical beamforming, Modern Phys. Lett. B (MPLB) 22 (2008) 1147–1151, https://doi.org/10.1142/S021798490801598X.
[206] A. Schmitt, L. Lamotte, Source identification inside cabin using inverse methods, in: 3rd Berlin Beamforming Conference – 3rd BeBeC, 2010.
[207] C. Nau, W. Moll, M. Pollow, M. Vorländer, Extension of traditional measurement methods in vehicle acoustics to the method of source localization in the vehicle interior, in: 5th Berlin Beamforming Conference – 5th BeBeC, 2014.
[208] P. Sijtsma, Green's functions for in-duct beamforming applications, in: 18th AIAA/CEAS Aeroacoustics Conference (33rd AIAA Aeroacoustics Conference), American Institute of Aeronautics and Astronautics, 2012, https://doi.org/10.2514/6.2012-2248.

[209] P. Sijtsma, Circular harmonics beamforming with multiple rings of microphones, in: 18th AIAA/CEAS Aeroacoustics Conference (33rd AIAA Aeroacoustics Conference), American Institute of Aeronautics and Astronautics, 2012, https://doi.org/10.2514/6.2012-2224.
[210] T. Suzuki, B.J. Day, Comparative study on mode-identification algorithms using a phased-array system in a rectangular duct, J. Sound Vib. 347 (2015) 27–45, https://doi.org/10.1016/j.jsv.2013.06.027.
[211] M. Park, B. Rafaely, Sound-field analysis by plane-wave decomposition using spherical microphone array, J. Acoust. Soc. Am. 118 (5) (2005) 3094–3103, https://doi.org/10.1121/1.2063108.
[212] R.P. Dougherty, W.D. Fonseca, S.N.Y. Gerges, Beamforming in reflecting environments: an experiment in a reverberation chamber, in: ASME 2008 Noise Control and Acoustics Division Conference, ASME, 2008, https://doi.org/10.1115/ncad2008-73020.
[213] E.C. Cabada, N. Hamzaoui, Q. Leclère, J. Antoni, Acoustic imaging applied to fault detection in rotating machine, in: Surveillance 8, International Conference – October 20–21, 2015, no. 8, 2015.
[214] J. Antoni, D. Abboud, G. Xin, Cyclostationarity in condition monitoring: 10 years after, in: 27th International Conference on Noise and Vibration Engineering, ISMA 2016, 2016, pp. 2365–2375.
[215] Q. Leclère, N. Hamzaoui, Using the moving synchronous average to analyze fuzzy cyclostationary signals, Mech. Syst. Signal Process. 44 (1–2) (2014) 149–159, https://doi.org/10.1016/j.ymssp.2013.01.005.